ADDIS ABABA INSTITUTE OF TECHNOLOGY

SCHOOL OF GRADUATE STUDIES

ASSESSMENT OF THE EFFECT OF CONCRETE CLASS VARIATION ON DYNAMIC RESPONSE OF FRAMED STRUCTURES

NATNAEL KEBEDE

MAY, 2011

ASSESSMENT OF THE EFFECT OF CONCRETE CLASS VARIATION ON DYNAMIC RESPONSE OF FRAMED STRUCTURES

BY

NATNAEL KEBEDE

A Thesis Submitted to the Graduate school of Addis Ababa Institute of Technology in partial fulfillment of Master of science in Civil Engineering

Addis Ababa

May, 2011

ADDIS ABABA INSTITUE OF TECHNOLOGY

SCHOOL OF GRADUATE STUDIES

DEPARTMENT OF CIVIL ENGINEERING

Assessment of the Effect of Concrete Class Variation on Dynamic response of Framed Structures

By

Natnael Kebede

May, 2011

Approved by Board of Examiners

Dr Shifferaw Taye	_____	_____
Advisor	Signature	Date
Dr Ing. Bedilu Habte	_____	_____
External Examiner	Signature	Date
Dr Ing. Girma Zerayohannes	_____	_____
Internal Examiner	Signature	Date
Melaku Mohammed	_____	_____
Chairman	Signature	Date

DECLARATION

I, the undersigned, declare that this thesis is my original work and has not been presented for a degree in any other university and that all sources of material used for the thesis have been duly acknowledged.

Candidate

Name: Natnael Kebede

Signature:

Faculty of Technology

Addis Ababa Institute of technology

Date of Submission: February, 2011

ACKNOWLEDGMENTS

Above all I should praise God for his provision on every aspect of the inputs, spiritual and material, necessary for the completion of the thesis. There is no doubt that a single step further is unthinkable without his involvement.

Next I would like to extend my deepest gratitude to my advisor Dr. Shifferaw Taye for his assistance. I am also grateful to all who were cooperative in completing the questionnaire without undue delay and those who furnished me with concrete test result data.

Finally I have to extend my appreciation to my family for providing the different facilities, for their uninterrupted support from the very beginning and for revising the write up and assistance in writing some of the manuscript.

CONTENTS

List of Figures ..... **vi**
List of Tables ..... **vii**
List of Appendices ..... **viii**
List of Symbols ..... **ix**
Abstract ..... **xi**
1 INTRODUCTION **1**
1-1 General 1
1-2 Statement of the problem. 3
1-3 Objective of the study 4
1-3-1 General objective 4
1-3-2 Specific Objective 4
1-4 Scope of the study 5
2 LITERATURE REVIEW **6**
2-1 General 6
2-2 Material and frame element modeling 6
2-2-1 Reinforced concrete under monotonic and cyclic loading 6
2-2-2 Reinforcement Bar under monotonic and cyclic loading 8
2-2-3 Hysteretic Behavior of reinforced concrete 9
2-3 Frame Member Modeling 11
2-3-1 Single component model 11
2-3-2 Multi component model 15
2-4 Background of the Analysis 16
2-4-1 Numerical Method for elastic systems 16
2-4-2 Non linear Numerical Method 18
2-4-3 Stiffness matrix formulation for elastic perfectly plastic beam element 19
3 ANALYSIS OF FRAME FOR SESIMIC LOADING **24**
3-1 General 24
3-2 Assumptions and Analysis Considerations 24
3-3 One Bay Moment Resisting Frame Analysis 25

3-3-1 Description of the model 25
3-3-2 Input Data 26
3-3-2-1 Material property 26
3-4 Moment rotation relation as verification for SAP out put 30
3-5 Result Discussion 36
3-5-1 One bay frame 37
3-5-2 Three bay moment resisting frame 43
3-5-3 Six Bay moment resisting Frame 45
4-CONCLUSION 51
5 RECOMMENDATION 53
REFERENCE 54
APPENDIX A 56
APPENDIX B 588

List of Figures

Figure 2-1 Idealised stress-strain diagram for steel subjected to cyclic loading. [11].....9
Figure 2-2 Hysteretic characteristics of reinforced concrete member. [8].....10
Figure 2-3 Inelastic rotation of beam: (a) moment; (b) curvature and inelastic rotation [8] 13
Figure 2-4 Multi component member model [8]. 16
Figure 2-5 Resisting force displacement diagram [1]. 18
Figure 2-6 Iteration with in a time step Newton-Raphson method [1]. 19
Figure 2-7 Elastic perfectly plastic Moment-rotation relationship of beam element.[9].....20
Figure 3-1 Stress strain relationship for confined concrete.....28
Figure 3-2 Artificial ground motion history.....29
Figure 3-3 Beam section and stress block of uncracked section. 30
Figure 3-4 Stress block distribution at first yielding of tension bar. 32
Figure 3-5 Comparison of results of SAP and Analytical Result 36
Figure 3-6 One bay three storey frame with possible plastic hinge location 37
Figure 3-7 Hinge result for hinge number one 38
Figure 3-8 First storey displacement.....39
Figure 3-9 Fiber result of fiber 4 beam hinge 2. 39
Figure 3-10 Base shear of three bay frames for the six cases.....44
Figure 3-11 Percentage difference for base shear of three bay frames 45
Figure 3-12 Percentage difference for column member moment of three bay frame.....45
Figure 3-13 Base shear six bay six storey frame. 46
Figure 3-14 Base moment six bay six storey frame.....47
Figure 3-15 Percentage difference for base shear and drift of six storey frames 47

List of Tables

Table 3-1 Summary of one bay three storey result ……..…….41
Table 3-2 Summary of six bay six storey result ……...……..…….48
Table 3-3 Summary of results……..…….……..……....50
Table A 3-1 Summary of one bay four storey result ……...…….58
Table A 3-2 Summary of one bay five storey result ….....…….…59
Table A 3-4 Summary of one bay six storey result …….....…..……..…..…….60
Table A 3-5 Summary of three bay three storey result …….……...……...61
Table A 3-5 Summary of three bay four storey result …….……..….62
Table A 3-6 Summary of thee bay five storey result ……..……63
Table A 3-7 Summary of three bay six storey result ……..…….…….64

List of Appendices

Appendix A Questionnaire ……...56
Appendix B One and three bay summary table……...……..58

List of Symbols

A_s	*Area of steel in compression*
A	*Area of concrete*
C	*Damping*
C_s	*Force in reinforcement bar of compression zone*
C_c	*Force in compressed zone of concrete*
d	*Concrete section depth*
E_s	*Elastic modulus of steel*
E_{co}	*Initial tangent modulus of elasticity of concrete*
ε_y	*Yield strain of reinforcement bar*
ε_{cl}	*Strain corresponding to* f_c
ε_{cu}	*Failure strain or maximum "usable" strain*
ε_{c50}	*Strain corresponding to 50% reduction in strength*
ε_{c20}	*Strain corresponding to 80% reduction in strength*
ε_{cm}	*Strain corresponding to maximum strength just at loading*
$\varepsilon_{s'}$	*Strain of compressed steel*
f_{ck}	*The characteristic cylinder strength of concrete*
f_c	*The cylinder strength of concrete*
f_s	*Force in reinforcement bar*
F	*Applied load*
h	*Concrete section width*

List of Symbols (continued)

I	*Area moment of inertia of gross concrete section*
k_i	*Initial tangent stiffness*
k_{sec}	*The secant stiffness*
K	*Neutral axis depth factor*
L	*Length*
m	*Mass*
M_{cr}	*Cracking moment of concrete section*
M_y	*Moment at first yield of steel in tension*
n	*Modular ratio*
p	*Ratio of post yield to elastic modulus*
T	*Force in tension steel*
u	*Displacement*
$\dot{u}$	*Velocity*
$\ddot{u}$	*Acceleration*
Z	*Slope of the declining region of stress strain relationship of concrete*
ρ	*Reinforcement ratio*
Δu	*Incremental displacement*
$\Delta \dot{u}$	*Incremental velocity*
$\Delta \ddot{u}$	*Incremental acceleration*
ΔF	*Incremental load*

Abstract

Most of the time attention is not given by engineers when higher quality of concrete than the design requirements is used. And this indeed will increase the stiffness. In order to study the behavior and response to such increased stiffness, moment resisting planar structure has been selected for the research. Parametric study was conducted by varying the number of bays, the number of storey and percentage of the total storey with which higher quality concrete is made. The higher class concrete was obtained from actual test data selected out of 1,148 results out of which 575 of them are the 28^{th} day strength. The mean plus one standard deviation value is selected for the 28^{th} day test result.

Time history analysis using Newmark's average acceleration method is used to obtain the response at different times. The result shows that higher response was observed in all the parametric cases as compared to what is obtained from uniform concrete class analysis.

CHAPTER ONE

1 INTRODUCTION

1-1 General

Structures subjected to earthquake induced ground motion experience a significant magnitude of lateral load. This depends on many factors which includes peak value and motion character of ground, natural period of vibration of the structure, damping ratio, structural arrangement, material property, support fixity, soil type, stiffness and mass of non structural part. The choice of analysis for seismic load is dictated by different factors. Though many building codes including Ethiopian building code allow the use of equivalent static analysis for regular structures, response spectrum or time history analysis is mandated as the irregularity both in plan and elevation manifested. Again with the expectation of medium to high seismic region inelastic seismic analysis is required. Therefore, equivalent static analysis is limited to analysis of regular structure, the regularity being with respect to plan, elevation, mass and stiffness distribution.

Among the parameters controlling the structural response to seismic excitation, stiffness of framed structure does depend on member's arrangement, member sections, joint rigidity, and material property (strength and stress strain relationship) and hysteretic behavior for nonlinear range of response. In this paper the effect of stiffness variation due to material strength variation will be assessed. The strength variation could be due to mix design, utilization of admixture or use of ingredients that yield high quality concrete. This could be the case when high quality ingredient is used such as crushed basalt is used as a fine aggregate.

Reinforced concrete structures designed according to present building codes as moment resisting frames to withstand strong earthquake motions are expected to deform well into the inelastic range and dissipate the energy input by the base motion through stable hysteretic behavior of structural components. The accurate prediction of the mechanical behavior of the structure during earthquake excitations depends on the development of reliable analytical models which describe the hysteretic behavior of these regions [7].

Better representation of the material property regarding the stress strain relationship and hysteretic behavior at the critical regions is necessary to closely capture the response up to failure. Efficient structural performance is achieved in addition to the modeling part by detailing for the design values in such a way that column elements remain in elastic range except at the base to avoid collapse mechanism by allowing hinging starts at the beam extreme points. Input energy at the base, for seismic load, should be taken up by good hysteretic performance of as many possible numbers of hinges as possible as [7]. For well designed and detailed moment resisting framed structures, the only concerning issue for severe seismic load is deterioration of stiffness which reduces the energy dissipation mechanism, increases the period and flexibility and induces redistribution of internal stress.

1-2 Statement of the problem.

A concrete test is one of the major tests conducted at construction phase of a given project. This is done by either performing prior test made before actual cast is made or after the concrete is cast by hammer test. Though the first method is the usual and more accurate way of determining the strength, result interpretation regarding higher test result is usually given less attention. Accepting high quality concrete tests will introduce stiffer structural members. And the involvement of these stiffer members will indeed bring about a differed seismic response according to structural dynamic theory.

The motivation for working on this title is due to the experience at a project site where crushed basalt was used as a fine aggregate instead of river sand. This resulted in a higher concrete strength than what was required at the design phase. It was used up to some floors until it was completely depleted and shifted to using river sand fine aggregate for the rest of the floors. Utilizing this higher strength concrete would definitely increase the stiffness of those structural members.

According to theory of structural dynamics, varying stiffness of structural members, given other parameter constant, will affect the response of the whole structure. Therefore, determining to what extent will the different action effects are sensitive gives the basis of decision on the need to control such high strength concrete. Based on the result, it will be a supportive document for a regulatory body to think of arranging awareness creation on test result interpretation.

1-3 Objective of the study

1-3-1 General objective

The objective of this paper is to show the effect on seismic response of using higher class concrete than specified during design stage. In light of this, the extent of variation of the different action effects will be assessed. Accordingly, to stipulate a benchmark for whether giving attention to test results depicting over strength is needed or not. Based on the result, it will act as a supportive document for possible decision to be made on the need for awareness creation.

1-3-2 Specific Objective

This paper has a specific objective of conducting parametric study on seismic response of planar moment resisting concrete framed structures. The parameters used for comparisons includes, number of storey, number of bays, percentage of total height at which either high or low class concrete is used below. It is aimed at comparing action effects for the above parameters and determining the most sensitive ones along with the extent of variation. This will be compared with uniform concrete class throughout the total height to clearly visualize the effect.

1-4 Scope of the study

This paper is limited to analysis of planar moment resisting concrete framed structures. A single seismic load developed from artificially generated ground motion history that best fits the response spectrum of EBCS-8 [4] is used. Concrete class variation is only in two regions that is, some percent of the storey is made with high class concrete and the rest with lower class (the design value). This scenario will be reversed and analyzed similarly. Two dimensional frames are chosen to easily see the effect by reducing the number of parameters involved in the analysis. In addition, the number of storey among the parameters is limited to six storeys as sections obtained for higher number of storey dictated the use of dual lateral load resisting system which is outside the scope of the thesis.

CHAPTER TWO

2 LITERATURE REVIEW

2-1 General

The development of reinforced concrete analysis to seismic load has been enhanced by the effort made by researchers especially since the last fifty years. This was made possible by closer modeling of material property, frame element and hysteresis behavior.

2-2 Material and frame element modeling

2-2-1 Reinforced concrete under monotonic and cyclic loading

Tests conducted on unconfined concrete compressive strength by monotonic load depict that higher strength concrete are less ductile than lower strength concrete while the ultimate strength is obviously higher. Thus, lower class concretes are more ductile than higher class showing larger ultimate strain. The stress strain relationship can be divided into three parts [11]. These are the initial (linear) part corresponding to the elastic range. The second part corresponds to the range of 70% up to 100% of the cylinder or prism strength. It is characterized by non linear material behavior with gradual tangent stiffness reduction. The third part represents the declining stage where the strain increases with decrease in stress. Though the maximum possible strain could go up to 1.0-1.5%, the conventional failure strain beyond which no further strain value is acceptable is limited in different codes. For instance Euro-code 2 Part one [6], Design of concrete, limits the value to 0.35% for $f_{ck} \le 50MPa$ which is similar to EBCS-2[3].

The best analytically and experimentally obtained results are represented by three regions [11]. For the ascending branch, Hognestad's parabola that best represents is given by :-

$$\sigma_c = f_c\left[\frac{2\varepsilon_c}{\varepsilon_{cl}} - \left(\frac{\varepsilon_c}{\varepsilon_{cl}}\right)^2\right] \qquad \ldots (2\text{-}1)$$

Where $\varepsilon_{cl} = \dfrac{2f_c}{E_{co}}$ is the strain corresponding to stress $\sigma_c = f_c$

f_c is the cylinder strength of concrete

E_{co} is the initial tangent modulus of elasticity.

For the descending branch, a straight line defined by two points corresponding to (ε_{cl}, f_c) and a point corresponding to a 50% reduction in strength. Curve fitting of experimental result has led to the following equation.

$$\varepsilon_{c50} = \frac{3 + 0.29 f_c}{145 f_c - 1000} \quad \ldots (2\text{-}2)$$

where f_c is in MPa

Hence, the equation of the descending branch will be

$$\sigma_c = f_c\left[1 - z(\varepsilon_{c-}\varepsilon_{cl})\right] \quad \ldots (2\text{-}3)$$

where $z = \frac{0.5}{\varepsilon_{c50} - \varepsilon_{cl}}$

The residual strength beyond this stage ranges from 20 to 30 percent of the ultimate strength according to different researchers.

When dealing with seismic behavior, rate of loading also affects the strength to the extent of 25% for normal concrete class less than 60MPa when the strain rate is 0.02/sec. And it is noted that typical values of strain rates induced by earth quake loads ranges b\n 0.01 to 0.02/sec [11]. Correlating stress strain results obtained from static load application for dynamic loading will in general give a more safe result regarding strength. Using the result for ultimate deformation however, will produce unsafe result due to an exaggerated deformation capacity obtained from static load test. That is higher strain rate will increase the material strength while it decreases the ductility making the concrete brittle as compared to the static response.

Concrete under reversed loading shows deterioration both in stiffness and ultimate strength once it has gone beyond the elastic range. It is shown in loading and unloading curves of experimental results [11]. In this regard, the ductility demand imposed by seismic ground motion affects the behavior of concrete structure. The envelope of the curve for reversed loading coincides with for monotonic loading except some deviations observed at larger strains [11].

Even though, researches made on unconfined concrete is useful to understand it's behavior seismic loading in general, additional information for concrete confined by transverse reinforcement is necessary to address the behavior by conducting tests on biaxial and tri axial tests.

Experiments show confinement of concrete increases its strength and ductility, therefore study made on confined concrete is relevant to capture its seismic behavior. The strength of concrete increases up to about 25% for a lateral confinement pressure coefficient of 0.5 and by 16% for equal uniaxial orthogonal loads i.e. confinement pressure coefficient of 1. For biaxial tensile load, the effect is insignificant while strength reduction has been observed in tensile transverse force [11].

2-2-2 Reinforcement Bar under monotonic and cyclic loading

Reinforcement bar used for reinforcing concrete members subjected to seismic load requires parameters for describing its behavior that depends on the percentage of carbon content. The most important characteristics defining the property of reinforcement bar are the yield strength, the ultimate strain and strength, strain hardening property and bond strength with surrounding concrete. High grade steel has more strain hardening but lesser ultimate strain than low grade steel. Accordingly, the use of lower grade with high ductility steel is recommended for seismic design of concrete structures. The reason is that limited post yield strength will enable plastic hinge be confined only at predefined localities of frame element. However, mild steel of high strength that has higher strain hardening will generate a higher moment at large strains. And this will induce a higher shear stress at the plastic hinge zone. Shear failure usually occur for designs that are based on capacity design philosophy where the post yield strength is not determined accurately.

For monotonic loading, elastic perfectly plastic idealization is sufficient for vertical load. But this idealization should be substituted by elasto-plastic with strain hardening property for seismic loading. This will enable one to determine the shear resistance of a frame section based on the ultimate flexural capacity of the same members. In this regard over strength factor, a factor for including post yield strength is used over and above the elastic-perfectly plastic.

It has also been inspected that monotonic and repeated loading coincides as observed in the case of concrete. Cyclic loading on steel, though the development of full compression in steel is difficult to achieve, shows stiffness degradation with non-linear number of cycles even at significantly lower stress level than yield stress. This property of material is known as Bauschinger effect. The unloading curve follows similar slope as the initial elastic range as shown in figure 2-1.

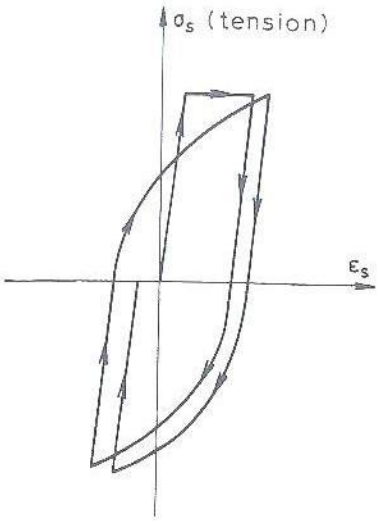

Figure 2-1 Idealised stress-strain diagram for steel subjected to cyclic loading. [11]

2-2-3 Hysteretic Behavior of reinforced concrete

To describe the behavior of RC members under cyclic load reversals phenomenological models of hysteretic behavior are typically used. While only a few parameters are needed to describe the hysteretic behavior when flexure governs the response, many more parameters become necessary in members with complex interactions of bending moments, shear and axial forces. These parameters are typically established from a limited set of experimental data making the general applicability of such models questionable. It appears doubtful that a single hysteretic model can approximate the actual behavior of RC regions over the wide range of possible interactions of bending moment, shear and axial force in structures subjected to earthquake excitations [7].

Reinforced concrete members subjected to large cyclic deformations are subjected to deterioration in both strength and stiffness with number of inelastic cycle and the extent of

inelastic range. This could also be observed in the post capping, unloading stiffness and reloading range in an accelerated manner [8].

This has been shown in the force deflection curve of a cantilever column. (a) Tensile cracking of concrete and yielding of longitudinal reinforcement reduced the stiffness; (b). The loading stiffness in the second cycle was lower than that in the first cycle, although the resistances at the peak displacement were almost identical; and (c) average stiffness (peak-to-peak) of a complete cycle decreased with a maximum displacement amplitude.

For example, the peak-to-peak stiffness of cycle 5, after large amplitude displacement reversals, was significantly reduced from that of cycle 2 at comparable displacement amplitude. Therefore, the hysteretic behavior of the reinforced concrete is sensitive to loading history.

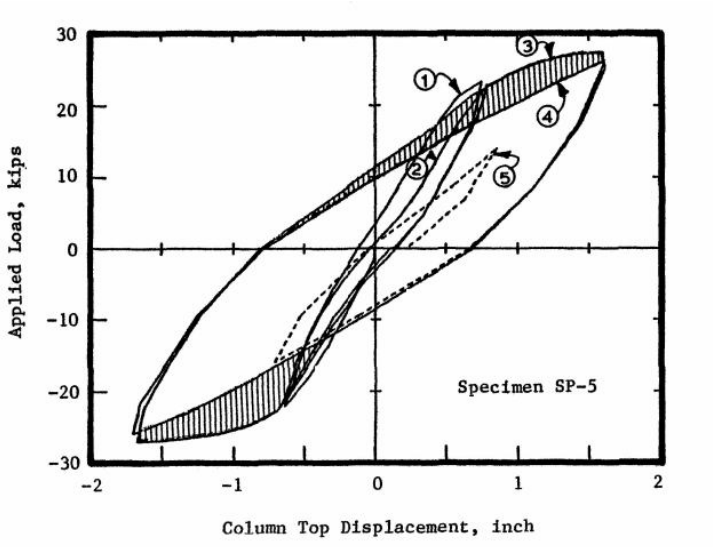

Figure 2-2 Hysteretic characteristics of reinforced concrete member. [8].

Different flexural hysteresis models have been proposed by researchers that are expected to be stable under the predicted displacement history.

a- Bilinear model

It is the simplest model among the category and elastic-perfectly plastic model has the advantage of computational simplicity than elastic with constant post yield stiffness. The modeling method does not incorporate stiffness degradation in higher cycles of reloading and unloading thereby not suitable for refined non linear analysis.

b- Takeda's Degrading stiffness model

It defines better the actual behavior of concretes as it is developed from experimental curve fitting. Yielding of reinforcement bar and cracking due to flexure is included for representing the stiffness deterioration, and strain hardening is also included in the model.

It also handles the unloading stiffness deterioration by introducing a rule that reduces the stiffness as a function of the previous maximum displacement. This model predominantly covers the flexural behavior neglecting shear and bond slip behavior or bond deterioration.

c- Degrading tri linear model

Before yielding it is similar to bilinear model after which it is a perfectly plastic behavior. Stiffness change is included as in Takeda at yielding and cracking with tri linear back bone curve. After the yield point up to the next (reversed displacement) yield point, it takes the form as bilinear with post yield constant strain hardening but in a reduced stiffness.

2-3 Frame Member Modeling

While most civil engineering framed structures subjected to low seismic load respond elastically, inelastic response will be induced by medium to high magnitude of earthquakes. Thus, the need to closely observe the behavior of nonlinear property is implied. Frame member modeling and frame section modeling in nonlinear range is important in addition to what is required for linear analysis.

2-3-1 Single component model

In this section different approaches to modeling frame member will be presented briefly. In general, frame member models can be categorized in three major parts. When presented from the simplest and crudest model to the much more refined and time consuming are: global model, discrete finite element, microscopic finite element models.

a-Global Model (lumped parameter model) - In this modeling technique non linear response at only predefined points of degrees of freedom are obtained. The output of this model is not to be relied on as it approximately represents the exact behavior especially for those seeking good

precision. In addition, difficulty in extracting the different response of members due to the limited number of degree of freedom makes its usage limited. However, global response determination such as ductility demand, storey displacement and drift are possible in this modeling technique.

b-Discrete Finite Element Model- In this approach assembled frame elements that describe the force deformation relation for reversed loading constitute the structural arrangement. These constitutive elements can be formulated as concentrated plasticity or distributed inelasticity except at regions where the element remains elastic.

i-Concentrated plastic hinge modeling- most of the time reinforced concrete frames exhibit inelasticity near extreme edges of structural members. An earliest approach to model such a phenomenon is concentrated plastic hinge zone of zero length which can be represented by nonlinear springs. The main advantage of lumped plasticity model is the simplicity of their formulation. Notwithstanding, these models oversimplify certain aspects of the hysteretic behavior, which may render them of limited applicability [5] The moment curvature hysteretic model that acts as a backbone curve of the section can be assigned in advance at the expected plastic hinge zones while limiting the remaining section in the elastic range. Though the dependency of hinge formation on frame curvature distribution exposed the method for critics, it still produces acceptable result for low storey structures. Among the lumped plasticity constitutive models proposed, some includes stiffness degradation in flexure and shear,' pinching' under load reversal and fixed end rotation at beam column joint interface to simulate the effect of bar pull-out [10]. When this model is used portion of the frame element other than the plastic hinge remains in the elastic zone.

Stiffness deterioration was first included by Giberson in 1969 which unlike Clough's model it was a one component model comprising two rotational springs with nonlinear property included [7]. All nonlinear deformations of the girder element are concentrated in these springs. This is an approximation of the real case where inelastic region is distributed inward from the extreme ends of a beam element. The merit of Giberson's model is, any hysteresis rule could be introduced through the rotational spring property in addition to its simplicity. This fact is also a weakness of the model because the member-end rotation should be dependent on the curvature distribution along the member, hence dependent on moments at both member ends [8]. Consider two cases of

moment distribution along a member AB with corresponding curvature distributions as shown in Fig 2-3. Inelastic rotations at the A end are given by the shaded areas. For the same moments at the A end, case II causes larger inelastic rotation at the A end. Consequently, this simple model does not simulate actual member behavior. Furthermore, it is not rational to lump all inelastic deformations at member ends.

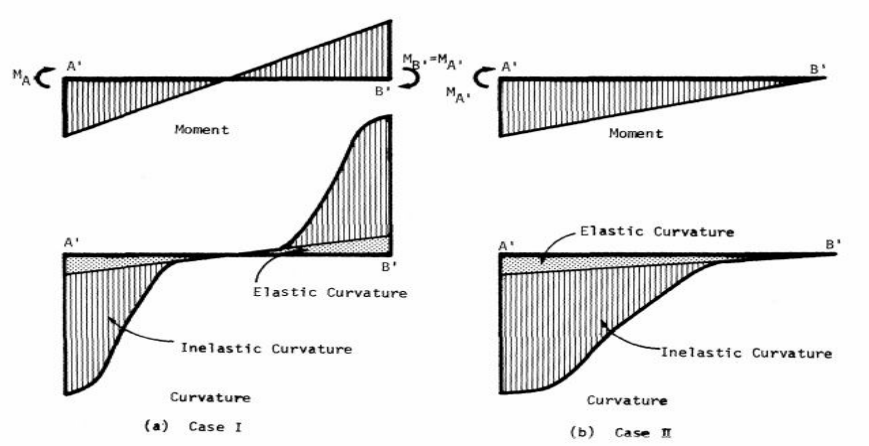

Figure 2-3 Inelastic rotation of beam: (a) moment; (b) curvature and inelastic rotation [8]

In Otani's model, the linear elastic element represents the entire elastic stiffness of the girder; the flexibility matrix of the inelastic element is derived as a function of the location of the point of contra flexure. This approach results in a non-symmetric flexibility matrix, unless one of the following assumptions is made: (a) the inelastic deformations are concentrated at the girder ends, or (b) the contra flexure point is assumed fixed at mid span of the member. Otani's study recognizes for the first time the importance of fixed-end rotations in predicting the seismic response of RC frame structures. Among the different hysteretic models used in the study the degrading tri linear connection model appears to be the most accurate [8]. It is also shown that the use of a degrading stiffness model results in an increase in inter story displacements which can have a substantial effect on the load carrying capacity of the structure due to the second order effect arising from high axial forces.

ii-Distributed inelasticity - A more accurate representation of frame element is achieved by using distributed inelasticity approach. The first model which accounts for the spread of inelastic deformations into the member was introduced by Soleimani et. al. [8]. A progressive inelastic deformation gradually spreads from the beam-column interface into the member while rest of the

beam remains elastic. The bond slip effect at the beam-column interface is modeled through lumped hinges which are located at member ends. These are related to the curvature at the corresponding end section through an "effective length" factor which remains constant during the entire response history.

A complete model for the analysis of seismic response of RC structures was proposed by Banon et. al.[8]. A single-component model in its original form describes the nonlinear behavior of the girder whose hysteretic moment-rotation rule is based on a modified Takeda model. In order to reproduce the "pinching" effect due to shear and bond slippage, a nonlinear rotational spring is inserted at each member end. The hysteretic model of the nonlinear springs is based on a bilinear skeleton curve with strength decay under large deformations and includes the effect of "pinching" during reloading.

An integrated experimental and analytical study on the effect of bond deterioration on the seismic response of RC structures was published by Otani et. al.[8]. The model adopted for beams and columns is the one-component model. Takeda's model is used to describe the hysteretic behavior of the elements. A rotational spring is inserted at each member end to model the slip of reinforcement due to bond deterioration; the hysteretic behavior of the spring is described by Takeda's model modified so as to account for the "pinching" effect during reloading. No strength decay is introduced in the monotonic skeleton curve, since experimental data did not provide such evidence.

In distributed inelasticity approach, the only input data to feed is material property and parametric characteristics of the element [10]. The cross-sectional behavior can be formulated either by discretising the cross- section into fibers “fiber model” or by using theory of plasticity in terms of stress – strain resultants. Members exposed to bending only in one direction can be modeled by layer element while those with bi axial bending a filament element is employed. In this method, the non linear shear deformation of filament is neglected assuming plain section remain plane. The section stress is determined from the summation of stress of each fibers that are defined by non linear stress strain relation initially. Section stiffness is determined from the aggregate effect of all fiber’s participation of the section while member element stiffness is calculated from the integration of all slice’s stiffness in the given element.

In between these two zones is the linear elastic element which is usually employed for part of frame element that is expected to behave elastically during the response history of the structure. In this section the yield strength of reinforcement is not exceeded thus a constant elastic modulus Ec is used. Constant stiffness along the span of an element is approximation because of varied longitudinal top and bottom reinforcement, differed level of cracking along the element and slab contribution for positive and negative bending. Different reduction factors may be assigned for flexure, shear, axial and torsional stiffness to account for micro cracks and bond slippage. For the study conducted in this paper reduction factors used for flexure, shear and axial are 0.7, 0.5 and 1 respectively.

***c-Microscopic Finite Element model*:-** Structural components are discretized into finite elements which represent elements, frame joints and material interface. Each element is interconnected at a finite number of nodes to represent the continuum solid. The level of refinement of the model depends on the required accuracy and on the available computational resources. While refined FE models might be suitable for the detailed study of small parts of the structure, such as beam-column joints, frame models are currently the only economical solution for the nonlinear seismic analysis of structures with several hundred members. In other words, member FE models are the best compromise between simplicity and accuracy, as they represent the simplest class of models that nonetheless manage to provide a reasonable insight into both the seismic response of members and of the structure as a whole [10].

2-3-2 Multi component model

More accurate method is achieved by decomposing the different stages of response of the given element critical section to define the hysteretic behavior. The very first inelastic girder model was proposed by Clough et. al. in 1965[7]. The model is based on two parallel beams one with elastic-perfectly plastic and the other with elastic beam to represent the post yield strain hardening property which replace the bilinear elastic-strain hardening force deformation relationship. This first model had limitation of including the stiffness degradation under cyclic loading .This multi component model comprises [10];

a- Linear elastic beam sub-element- similar property is used as discussed above for single element model for elastic portion of the element.

b- Rigid plastic hinge model – It represents the post yield property of the critical region. This can be categorized into two; as concentrated plastic hinge and distributed plastic element. The difference from what is discussed above is the two hinges at the extreme edges are connected by infinitely rigid bars. In this case the flexibility matrix is diagonal. When combined with the linear elastic model in part (a) it will give a non diagonal flexibility matrix that represents the element behavior excluding effect of shear deformation, shear sliding, fixed end rotation and bond slip. A member end rotation depends on both member and moments, Aoyana and Supano (1968) adapted a two component model, creating the multi different yield level at two member ends, and strain hardening [8].

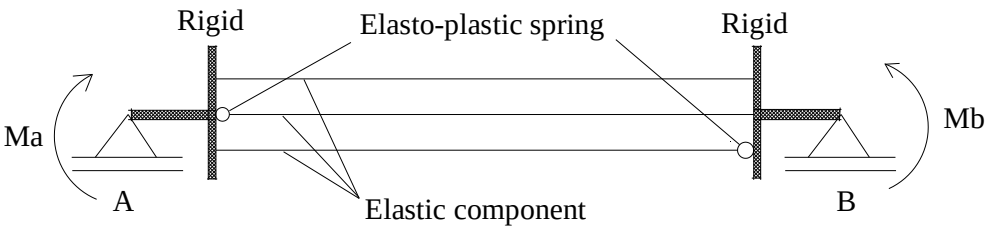

Figure. 2-4 Multi component member model [8].

2-4 Background of the Analysis

2-4-1 Numerical Method for elastic systems

The most general approach for solving the dynamic response of structural systems is the direct numerical integration of the dynamic equilibrium equations [14]. This method assesses the response at an incremental time which is most of the time constant to reduce the computational complexity. Equilibrium of the dynamic equation is made satisfied at the beginning of each time step during which the incremental response is evaluated to add up to the previous step response. The time step size is such that the stiffness and damping remains constant where as the nonlinear property is incorporated by revising the stiffness value at the beginning of each time step. Results

such as displacement, velocity or acceleration of the previous step are used as an initial value to the succeeding step.

Among the number of methods used, Newmark's methods that are the average acceleration and linear acceleration methods are the most popular. During the time step Δt, acceleration is assumed to remain constant with an average value of that at the beginning and end of the step for average acceleration method while linear variation during the time step is assumed for linear acceleration method. Linear acceleration is more accurate than average acceleration method for equal time step assessment [9].

Before proceeding to the steps employed in average acceleration method, the stability and accuracy of the two methods should be observed. The average acceleration method is unconditionally stable for any time step size but the size should be limited to achieve accuracy. The linear acceleration is conditionally stable that is it is stable for $\Delta t < 0.551Tn$ [1].

2-4-1-1 Newmark's average acceleration method

The average acceleration method assumes average acceleration during a single time step. In addition, property of systems, stiffness and damping could take any form of nonlinearity [9]. Thus it is not necessary for the stiffness and damping force be specified as a function of displacement and velocity respectively. It is required only to evaluate the coefficients every time Δt is changed.

The procedure is repeated after completing (obtaining the necessary values) the current time step and using the values as initializing data for the succeeding step. The two approximations that induce error are average acceleration assumption and constant stiffness and damping for a time step. These errors definitely accumulate with number of steps that however could be minimized by selecting a short time step size and conducting a total dynamic equilibrium at every step by expressing the acceleration using the differential equation of motion in which the displacement and velocity as well as stiffness and damping forces are evaluated at each time [9].

As stated in the previous paragraph, the choice of time step is important in minimizing the error accumulated. This is affected by the natural period of the structure, the variation of loading with time, the stiffness and damping complexity of the structure [9]. In general it has been found that sufficiently accurate results can be obtained if the time interval taken to be no longer than one

tenth of the natural period of the structure. The second consideration is that the interval should be small enough to represent properly the time variation of load.

2-4-2 Non linear Numerical Method

Nonlinearity makes a problem more complicated because equations that describe the solution must incorporate conditions not fully known until the solution is known-the actual configuration, loading, condition, state of stress, and support condition. The solution cannot be obtained in a single step of analysis. We must take several steps, update the tentative solution after each step, and repeat until a convergence test is satisfied. The usual linear analysis is only the first step in this sequence [2].

The Newton-Raphson method is the most rapidly convergent process for solution of problems in which only one evaluation of stiffness is made in each iteration. Of course this assumes that the initial solution is within the zone of attraction and thus diversion does not occur [15].

Inelastic system equation is modified from elastic system equation by the second and the last term which is the resisting force and system damping. The stiffness is dependent on the displacement, velocity and the prior loading history of the system once it has gone beyond the elastic range.

$$-m\ddot{u}_g = m\ddot{u}_i + c_i\dot{u}_i + f_s(u_i, \dot{u}_i) \qquad \ldots \text{ (2-4)}$$

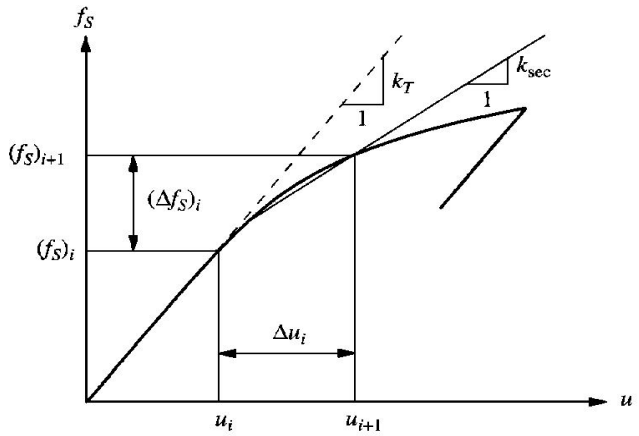

Figure 2-5 Resisting force displacement diagram [1].

The incremental equilibrium equation is

$$-m\Delta\ddot{u}_g = m\Delta\ddot{u}_i + c_i\Delta\dot{u}_i + \Delta f_s(u_i, \dot{u}_i) \qquad \ldots(2\text{-}5)$$

The incremental resisting force as shown in the figure 2-5 is $k_{\text{sec}}\Delta\dot{u}_i$ but the tangent modulus at the beginning of the time step could be used instead of the secant modulus. Using this stiffness value of Δk_t in equation 2-5 will lead to a similar equilibrium equation as for elastic system.. The only additional step to be followed is to update the k_t at the beginning of each time increment. Each step requires an iterative process to arrive at the incremental displacement and hence the force as shown in figure 2-6.

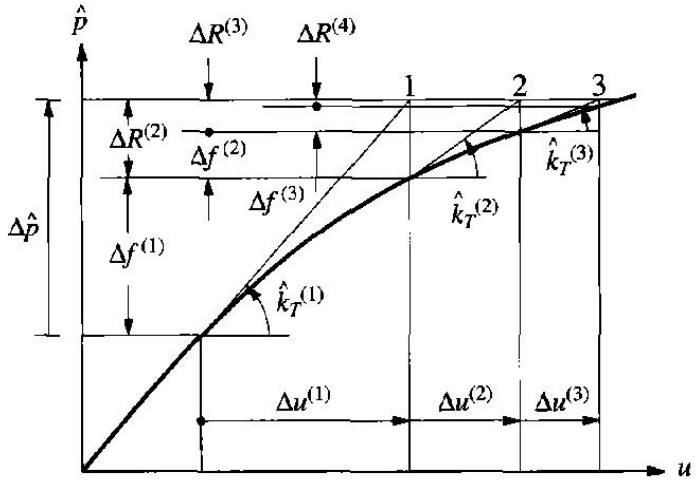

Figure 2-6 Iteration with in a time step Newton-Raphson method [1].

2-4-3 Stiffness matrix formulation for elastic perfectly plastic beam element

Beam elements whose deformation is only due to flexure or with negligible axial force deformation as compared with flexural deformation are assessed. The force deformation relation of elastic perfectly plastic idealization is used in this section along with the assumption that deformations are small and plane sections remain plane before and after loading. Elastic beam theory dictates that beam displacement interpolation functions corresponding to the four degrees of freedom for beams subjected to loading in two dimension are one displacement and one rotation at each of the two nodes are:-

$$\psi_1(x) = 1 - 3\left(\frac{x}{L}\right)^2 + 2\left(\frac{x}{L}\right)^3 \quad \ldots(2\text{-}6)$$

$$\psi_2(x) = x\left(1 - \frac{x}{L}\right)^2 \quad \ldots(2\text{-}7)$$

$$\psi_3(x) = 3\left(\frac{x}{L}\right)^2 - 2\left(\frac{x}{L}\right)^3 \quad \ldots(2\text{-}8)$$

$$\psi_4(x) = \frac{x^2}{L}\left(\frac{x}{L} - 1\right)^2 \quad \ldots(2\text{-}9)$$

Displacement function 2-6 and 2-8 are deformed shapes corresponding to a unit displacement at the two nodes whereas 2-7 and 2-9 are the corresponding deformed shape functions due to unit rotation of the two nodes.

The stiffness coefficient for beams under flexure is given by

$$k_{ij} = \int_0^L EI\psi_i''(x)\psi_j''(x)dx \quad \ldots(2\text{-}10)$$

Where $\psi_i''(x)$ and $\psi_j''(x)$ are the displacement functions.

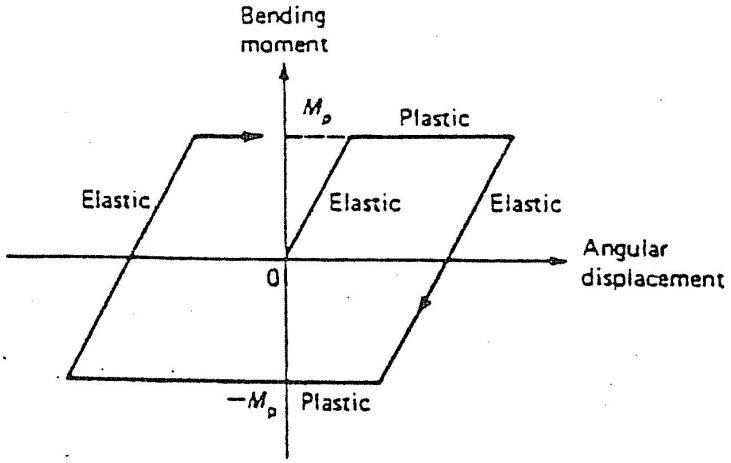

Figure 2-7 Elastic perfectly plastic Moment-rotation relationship of beam element.[9]

For beam of hinge formed at one end with hinge moment rotation relationship shown in figure 2-7 the displacement functions are modified as follows;

$$\psi_1(x) = 1 - \frac{3x}{2L} + \frac{x^3}{2L^3} \quad \ldots(2\text{-}11)$$

$$\psi_2(x) = 0 \quad \ldots(2\text{-}12)$$

$$\psi_3(x) = \frac{3x}{2L} - \frac{x^3}{2L^3} \quad \ldots(2\text{-}13)$$

$$\psi_4(x) = -\frac{x}{2} - \frac{x^3}{2L^2} \quad \ldots(2\text{-}14)$$

The stiffness coefficient k_{44} is obtained according to equation 2-10 by differentiating $\psi_4(x)$ twice , taking the square and integrating along the beam length L hence;

$$k_{44} = \int_0^L \left(\frac{-6x}{2L^2}\right)^2 dx = \frac{3L^3 EI}{L^4} = \frac{3EI}{L}$$

Similarly all other coefficients are evaluated and the stiffness matrix and the incremental equation will be obtained in the following form;

$$\begin{bmatrix} \Delta F_1 \\ \Delta F_2 \\ \Delta F_3 \\ \Delta F_4 \end{bmatrix} = \frac{EI}{L^3} \begin{bmatrix} 3 & 0 & -3 & 3L \\ 0 & 0 & 0 & 0 \\ -3 & 0 & 3 & -3L \\ 3L & 0 & -3L & 3L^2 \end{bmatrix} \begin{bmatrix} \Delta u_1 \\ \Delta u_2 \\ \Delta u_3 \\ \Delta u_4 \end{bmatrix} \quad \ldots (2\text{-}15)$$

The diagonal stiffness element k_{22} and all elements in the row and column are zero. This implies that joint rotation where the hinge is formed has no influence on other degrees of freedom. In addition, the incremental rotation Δu_2 at the plastic hinge is the incremental joint rotation not the rotation just at the neighborhood of the hinge in the elastic zone of the beam.

Similar procedure is followed for hinge formed at the other extreme end as shown in figure 2-8 and the incremental equation will take the form;

$$\begin{bmatrix} \Delta F_1 \\ \Delta F_2 \\ \Delta F_3 \\ \Delta F_4 \end{bmatrix} = \frac{EI}{L^3} \begin{bmatrix} 3 & 3L & -3 & 0 \\ 3L & 3L^2 & 3L & 0 \\ -3 & -3L & 3 & 0 \\ 0 & 0 & 0 & 0 \end{bmatrix} \begin{bmatrix} \Delta u_1 \\ \Delta u_2 \\ \Delta u_3 \\ \Delta u_4 \end{bmatrix} \quad \ldots (2\text{-}16)$$

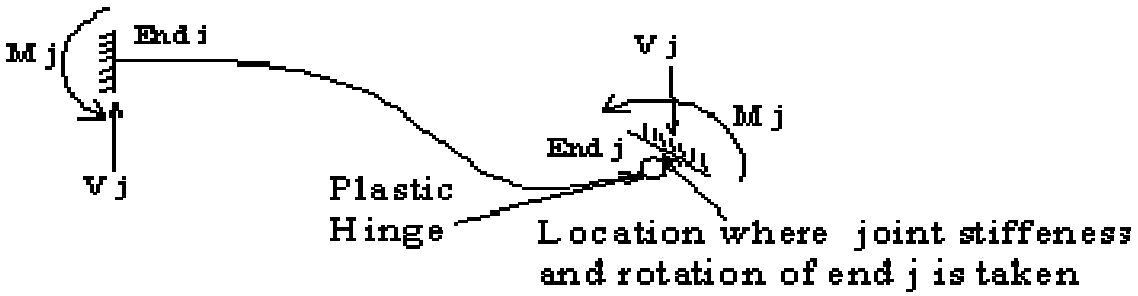

Figure 2-8 Elastic perfectly plastic beam element with plastic hinge

For hinge formed at both ends of the beam the theoretical result for the incremental force displacement relationship in matrix form is

$$\begin{bmatrix} \Delta F_1 \\ \Delta F_2 \\ \Delta F_3 \\ \Delta F_4 \end{bmatrix} = \frac{EI}{L^3} \begin{bmatrix} 0 & 0 & 0 & 0 \\ 0 & 0 & 0 & 0 \\ 0 & 0 & 0 & 0 \\ 0 & 0 & 0 & 0 \end{bmatrix} \begin{bmatrix} \Delta u_1 \\ \Delta u_2 \\ \Delta u_3 \\ \Delta u_4 \end{bmatrix} \qquad \ldots (2\text{-}17)$$

All elements in the stiffness matrix is zero due to our assumption at the beginning that post yield strength is zero that is elastic perfectly plastic section property is assumed. Had it been the case of post yield strength being some percent of the elastic stiffness, the matrix will take the form as follows :-

$$\begin{bmatrix} \Delta F_1 \\ \Delta F_2 \\ \Delta F_3 \\ \Delta F_4 \end{bmatrix} = p * \frac{EI}{L^3} \begin{bmatrix} 3 & 3L & -3 & 3L \\ 3L & 3L^2 & 3L & -\frac{3}{2}L^3 \\ -3 & -3L & 3 & -3L \\ 3L & -\frac{3}{2}L^3 & -3L & 3L^2 \end{bmatrix} \begin{bmatrix} \Delta u_1 \\ \Delta u_2 \\ \Delta u_3 \\ \Delta u_4 \end{bmatrix} \qquad \ldots (2\text{-}18)$$

where p is the ratio of post yield stiffness to elastic stiffness.

The incremental load induces additional rotation once plastic hinge is formed and this is equal to the addition in the difference between frame joint rotation and the beam element incremental rotation in the beam elastic zone just next to plastic hinge.

Elastic member stiffness matrix for beam column element

For beam-column member where significant axial load exists as compared with flexural stress, the elastic stiffness matrix would be six by six symmetric matrix. The axial load interaction is incorporated by using global stiffness matrix that is obtained from the direct stiffness matrix of the member.

$$\begin{bmatrix} \frac{EA_X}{l}C^2{}_X + \frac{12EI_Z}{L^3}C^2{}_Y & \left\|\frac{EA_X}{l} - \frac{12EI_Z}{L^3}\right|C_xC_Y & \frac{-6EI_Z}{L^3}C_Y & -\frac{EA_X}{l}C^2{}_X + \frac{12EI_Z}{L^3}C^2{}_Y & -\left\|\frac{EA_X}{l} - \frac{12EI_Z}{L^3}\right|C_xC_Y & -\frac{6EI_Z}{L^3}C_Y \\ . & \frac{EA_X}{l}C^2{}_X + \frac{12EI_Z}{L^3}C^2{}_Y & \frac{6EI_Z}{L^3}C_x & -\left\|\frac{EA_X}{l} - \frac{12EI_Z}{L^3}\right|C_xC_Y & -\frac{EA_X}{l}C^2{}_X - \frac{12EI_Z}{L^3}C^2{}_Y & \frac{6EI_Z}{L^3}C_x \\ . & . & \frac{4EI_Z}{L^3} & \frac{6EI_Z}{L^3}C_Y & -\frac{6EI_Z}{L^3}C_x & \frac{2EI_Z}{L^3} \\ . & . & . & \frac{EA_X}{l}C^2{}_X + \frac{12EI_Z}{L^3}C^2{}_Y & \left\|\frac{EA_X}{l} - \frac{12EI_Z}{L^3}\right|C_xC_Y & \frac{6EI_Z}{L^3}C_Y \\ . & . & . & . & \frac{EA_X}{l}C^2{}_X + \frac{12EI_Z}{L^3}C^2{}_Y & \frac{6EI_Z}{L^3}C_x \\ . & . & . & . & . & \frac{4EI_Z}{L^3} \end{bmatrix}$$

……..2-19

Where: C_x - Cosine of the angle b\n axis of the member and the axial load applied

C_y - Sine of the angle b\n axis of the member and the axial load applied

CHAPTER THREE

3 ANALYSIS OF FRAME FOR SESIMIC LOADING

3-1 General

Justification for the relevance of this thesis was supported by the questionnaire attached in appendix A that was completed by Engineers who are involved in contract administration and supervision. The questionnaire has covered attitudes from a wide range of experience from less than three years to more than 12 years of experience in the field. Accordingly, from the total who responded, 93.75% of them would accept higher concrete test result while only 6.25% would reject and order another trail batch test to be conducted. Therefore the need to analyze the response of higher strength concrete will be relevant as it is the core concept of the thesis.

In this chapter different moment resisting frames are analyzed using SAP 2000[16] to see the effect of stiffness variation arising from the change in concrete strength along the storey. Frame element sections are obtained by analyzing the frame for seismic loading by equivalent static analysis method with maximum bed rock acceleration of 0.1g which is recommended for zone 4 region of the country according to EBCS-8[4]. In addition, importance factor of 1.4 is used. The higher concrete class used has a 41.06 MPa ultimate strength that was obtained from the mean plus one standard deviation value of the 575 test results data. The lower class is 25 MPa is the characteristic compressive strength. The frame dimensioned accordingly will be loaded with a single ground motion history. The material nonlinearity, geometric nonlinearity and hysteretic behavior is introduced to the analysis to check whether the linear range is exceeded or not. The in-plane lateral earthquake force is an artificially generated ground motion history from response spectrum curve of EBCS-8 [4].

3-2 Assumptions and Analysis Considerations

The analysis approach used is non linear time history seismic analysis using Newmark's average acceleration method with alpha 0.5 and beta 0.25 values. A predefined locality of plastic hinge is determined with distributed plastic approach. Cracked sections are taken care of by corresponding stiffness reduction factor for shear and bending moment on beam elements. These

factors are introduced at early stage of analysis where frame section is defined. The assumption and considerations for analyzing the structure are:-

1- Members size is obtained based on equivalent static analysis (ESA)
2- Distributed plastic hinge is assumed at ends of members with joint strength higher than flexural strength of member elements
3- Fixed and rigid support reaction at the base
4- Equivalent structural damping of 5% is taken
5- P-Δ effect that is geometric nonlinearity effect is included
6- Moment-curvature relation is included based on fiber integration of those member sections designed using ESA.
7- Manually calculated moment-curvature relationship based on nonlinear material property of concrete and reinforcement bar is used to cross check the output result of a hinge
8- A single ground motion history that produces the design spectrum given on EBCS-8 [7] is used
9- Planer frame is used throughout the study
10- Perfect bond between concrete & steel i.e. no bond sleep deformation
11- Interaction of infill materials is neglected.
12- Axial deformation are neglected by assuming beams as part of the rigid diaphragm.
13- Stiffness character is not changed during each time step but it is revised at the beginning of every step by taking the last iteration result of the previous step.
14- Takeda's hysteresis rule of cyclic force-deformation relation is used.
15- Shear deformation is neglected.

3-3 One Bay Moment Resisting Frame Analysis

3-3-1 Description of the model

The frame comprise a 6m bay length & 3m story height –loads are transferred from the slabs tributary area including self weight of slab and finishing materials in addition to wall load. The analysis is first done by equivalent static analysis (ESA) to determine section size and reinforcement required. This structure is subjected to artificial ground motion history that produces the response spectrum curve recommended by EBCS-8[4]. The effect of cracking on stiffness of frame elements is taken care by introducing

reduction factors for different action effects; flexure, shear and axial force. Fiber element model is assigned at selected beam and column localities where plastic hinge is expected and where the result is to be assessed. Numerical time stepping method using Newmark's average acceleration method is used for nonlinear time history analysis. Five cases are used in this analysis category. These are uniform concrete class, the bottom 33% (one storey) high class concrete, the bottom 66% (two storey) high class concrete and the last two cases reversed are analyzed for three storey frame. Similar structural arrangement but with adjusted beam and column section as dictated by the static load analysis is used in the analysis of the other storey. The percentage is modified for four, five and six storey frames. That is 25% and 75% for four storey, 40 %and 60% for five storeys whereas 33% and 66% is used for six storey which is similar to the three storey. Storey shear at interface, storey moment at interface, storey drift at interface, base shear and base overturning moment are used for this parametric study. A total of 1148 concrete test results are collected to determine the mean and mean plus one standard deviation values. Out of these data 573 are 7 days test result while 575 are 28 days result. For the purpose of result refinement, the mean plus one standard deviation, that is 41.06MPa, of the 28^{th} day test result is used as the higher class concrete.

3-3-2 Input Data

3-3-2-1 Material property

a- Concrete - 25MPa concrete cube compressive strength with stress stain property of the monotonic loading that envelops the cyclic loading is chosen. Hence, hysteretic behavior of confined concrete is the same as that of unconfined concrete except for the envelope curve which is modified by confinement index K.

$$f_{cc} = kf_c$$

$$\varepsilon_{cc1} = k\varepsilon_{c1}, \text{ or } k_2\varepsilon_{c1}$$

where $\varepsilon_{c1} = 0.2\%$

$$k = 1 + \frac{\rho_w f_{yw}}{f_c}$$

ρ_w = volumetric ratio which is the ratio of volume of

confining hoop to confined core.

For region AB: $\varepsilon_c \le 0.002k$

$$f_c = f_{cc}\left[\frac{2\varepsilon_c}{0.002k} - \left[\frac{\varepsilon_c}{0.002k}\right]^2\right]$$

Region BC $0.002k \le \varepsilon_c \le \varepsilon_{cc20}$

$$f_c = f_{cc}\left[1 - Z(\varepsilon_c - 0.002k)\right]$$

where $Z = \dfrac{0.5}{\varepsilon_{cc50} - \varepsilon_{cc1}}$

$$\varepsilon_{cc50} = \frac{3 + 0.29 f_c}{145 f_c - 1000} + 0.75\rho_w\left(\frac{b_c}{s}\right)^2$$

where b_c - size of the confined concrete measured to the centroid of the peripheral hoop.

S-300 and C-25 is used for analyzing the structure using SAP 2000 [16]. Preliminary section size and reinforcement area is determined from elastic analysis to be b/h of 400mmx300mm with shear reinforcement of Φ8 c/c 150mm and longitudinal reinforcement of 8 Φ16.

$$\rho_w = \left[\frac{\Pi \times 8^2}{4}\right][400 - 25] \times 4 / [400 - 25 \times 2 - 6/2 \times 2] \times 150 = 0.00305$$

$$\varepsilon_{cc50} = \left[\frac{3 + 0.29 \times 20}{145(200 - 1000)}\right] + 0.75 \times 0.00317\left[\frac{359 - 50 - 6}{150}\right]^{0.5}$$

$$= 4.63 \times 10^{-3} + 3.33 \times 10^{-3}$$

$$= 7.66 \times 10^{-3}$$

$$Z = \frac{0.5}{7.96 \times 10^{-3} - k\varepsilon_{c1}} \quad \text{but} \quad K = 1 + 0.00317 \times \frac{300}{20}$$

$$Z = \frac{0.5}{7.96 \times 10^{-3} - 1.047 \times 0.002}$$

$$Z = 85.27$$

For region AB; i.e. $\varepsilon_{cc} < 0.002 \times 1.047 = 0.0021$

$$f_c = 20 \times 1.047\left[\frac{2\varepsilon_c}{0.0021} - \frac{\varepsilon_c{}^2}{0.0021^2}\right]$$

$$f_c = 20.95\left[\frac{2\varepsilon_c}{0.0021} - \frac{\varepsilon_c{}^2}{0.0021^2}\right]$$

For region BC;

$$f_c = 20.95\left[1 - 85.27(\varepsilon_c - 0.0021)\right]$$

Thus, the stress strain relationship to be used for concrete material property is as shown below in figure 3-1.

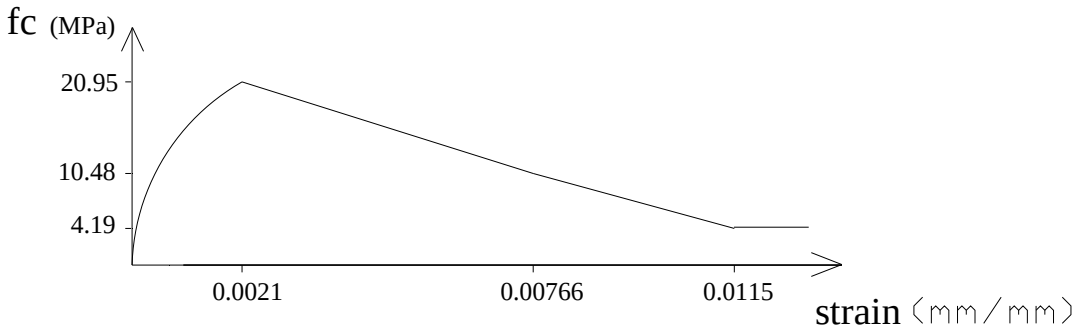

Fig 3-1 Stress strain relationship for confined concrete.

The strain corresponding to an 80% reduction from the ultimate strength is obtained as:-

$$\varepsilon_{cc}20,\ f_{cc20} = f_{cc}\left[1 - Z(\varepsilon_{cc20} - 0.002K)\right]$$

$$\frac{4.19}{20.95} = \left[1 - Z(\varepsilon_{cc20} - 0.0021)\right]$$

$$0.2 = \left[1 - 89.83(\varepsilon_{cc20} - 0.0021)\right]$$

$$\varepsilon_{cc20} = 0.0115$$

Takeda rule for hysteretic behavior is employed in the analysis of concrete material.

b- Steel reinforcement bar of grade s-300 is used in analyzing the frames. A single loading surface is insufficient as constitute model for use in dynamic or cyclic

analysis. Additional information is needed to develop the incremental constitutive relation that describes the stress strain paths in the fine distinct regimes that characterize a full loading cycle, which are elastic responses, pre-peak hardening, post-peak softening, elastic-plastic unloading and finally elastic-plastic [11].

3-3-2-2 Loading

Planar frame is extracted from a three dimensional frame of slab panel dimension of 6m by 6m. A solid slab is used with six meter span beam with load shared according to the corresponding tributary area.

Seismic load – Artificially generated ground motion history that could best fit the design response spectrum of EBCS-8 [4] is used as x-direction seismic load. Artificial ground motion history in terms of acceleration shown below is loaded to the structure but with scale factor of 0.14 which is computed from importance factor of 1.4, ductility class low, seismic zone 4, response factor of 2.5 for period less than 0.65 second. The load is applied for 10 seconds after the full application of dead and live load. The dead and live loads are applied as a ramp function of sufficient time to assure the load is static. In this regard different time for ramp load is assigned by comparing the fundamental period of vibration of each structure. The result is assessed until the 15^{th} second from the commencement of ground motion.

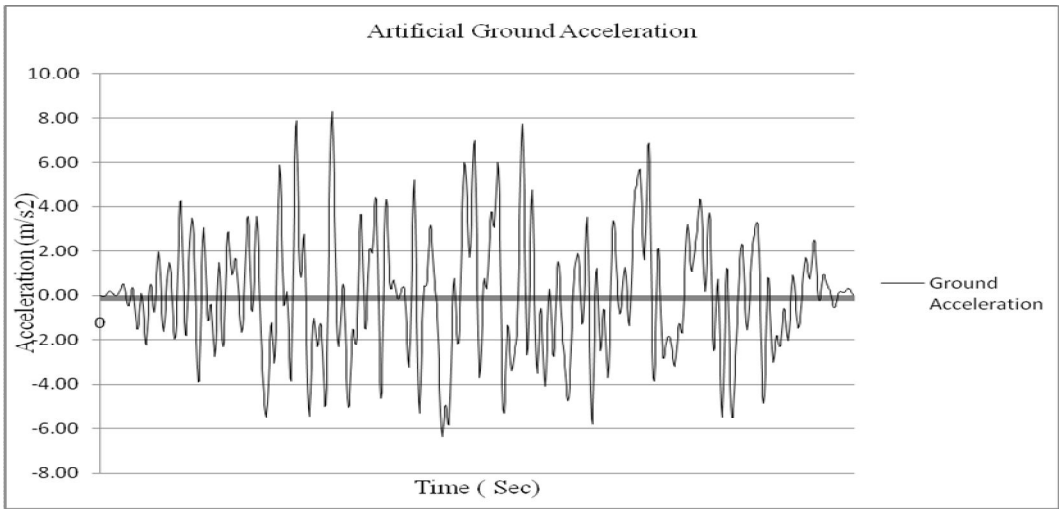

Figure 3-2 Artificial ground motion history

3-4 Moment rotation relation as verification for SAP out put

The location of plastic hinge can be located at some critical points of the frame. The moment rotation relationships of these critical sections are necessary as one of the inputs to the analysis. It is determined either by using the fiber element modeling of the section which is built in the software or by user defined force-deformation relation of the hinge section. For the purpose of cross checking the fiber element model of the software used, manual calculation is performed on the beam section already determined from the equivalent static analysis.

Therefore, the most probable points expected to yield is defined a priori. Hence beam elements are made up of one central elastic element bounded by two plastic hinge elements. The bottom most column sections are composed of elastic section below which plastic section is located.

Beam cross section $\frac{d}{h} = \frac{400}{300} mm$

Reinforcement bar $5\phi 20 = 1407 mm^2$ bottom reinforcement

$4\phi 20 = 1127 mm^2$ top reinforcement

$$\rho_{bot} = \frac{A_s}{bd} = \frac{1407}{[300 \times 357]} = 0.01314$$

$$\rho_{top} = \frac{A_s}{bd} = \frac{1127}{[300 \times 357]} = 0.0105$$

a - For Msd =< Mcr i.e. before cracking of concrete;

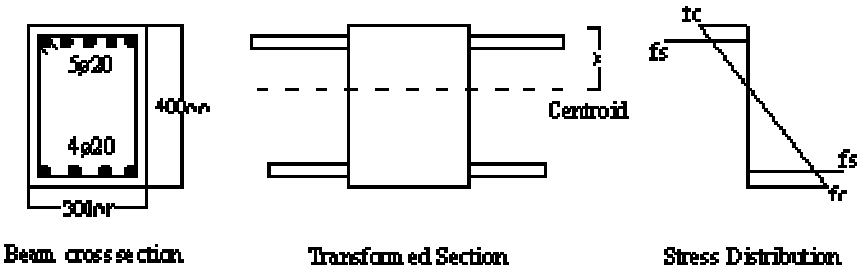

Figure 3-3 Beam section and stress block of uncracked section.

Modular ratio $n = \frac{E_s}{E_c} = \frac{200}{29} = 6.9$

Area $A = b \times h + (n-1)(A_s + A_s')$

$= 300 \times 400 + (6.9-1)(1407+1127)$

$= 134{,}950 mm^2$

The centroid of the transformed section

$$\bar{Y} = \frac{[120{,}000 \times 200 + 5.9 \times 1127 \times 357 + 5.9 \times 1407 \times 43]}{134{,}950}$$

$$\bar{Y} = \frac{[24{,}000{,}000 + 2{,}373{,}800 + 356{,}955.9]}{134{,}950}$$

$$\bar{Y} = 198.08 mm$$

Area moment of inertia

$$I_g = \frac{300 \times 400^3}{12} + 300 \times 400[200 - 198.08]^2 + 5.9 \times 1127[357 - 198.08]^2 + 5.9 \times 1407[198.08 - 43]^2$$

$$= 1.6 \times 10^9 + 442{,}36.8 + 167.93 \times 10^6 + 199.6 \times 10^6$$

$$= 1.9676 \times 10^9 mm^4$$

Modulus of rupture

$$f_r = 1.7 f_{ctk}$$

where $f_{ctk} = 0.21 f_{ck}^{2/3} = 1.55 MPa$

$$f_r = 1.7 \times 1.55 = 2.63 MPa$$

Cracking Moment

$$Mcr = \frac{f_r \times I_g}{\bar{y}_{bott}} = \frac{[2.63 \times 1.9676 \times 10^{-3}]}{[400 - 198.08]} = 25.62 KNm$$

Rotation

$$\frac{f_r / E_c}{\bar{y}_{bott}} = \frac{2.63/29 \times 10^3}{[400 - 198.08]} = 0.45 \times 10^{-6} rad/mm$$

But $$\chi = \frac{d^2\psi}{dx^2} = \frac{M}{EI} = \frac{\sigma I}{yEI}$$

$$\Rightarrow \frac{f_r}{yE} = \chi = \frac{\varepsilon}{y} = \frac{\Delta x}{Ly}$$

$$\Rightarrow \frac{\theta}{L} = \chi \quad \text{for one meter length, } \theta = \chi$$

Therefore, $0.45\times10^{-6}\, rad/mm = 0.45\times10^{-3}\, rad/m = \theta$

b - After cracking but at first yield

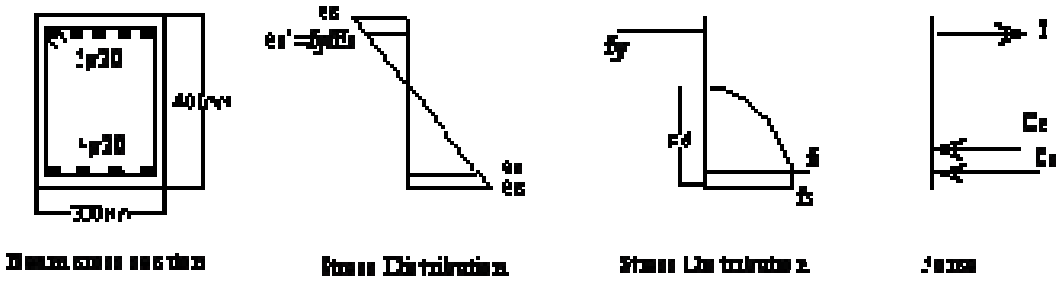

Figure 3-4 Stress block distribution at first yielding of tension bar.

The neutral axis depth factor is obtained by equating the summation of forces across the given section. For beam section the axial load P is approximately close to zero as compared to bending moment and shear force. Thus,

The force in the compressed concrete is;

$$Fc = \int_0^x 20.95[2(\frac{y}{0.002095[d-y]})]\varepsilon_x - [\frac{y^2}{0.002095^2[d-y]^2}]\varepsilon_y{}^2\, dy$$

From strain distribution,

$$K = \frac{y}{d}, \quad \frac{\varepsilon_c}{\varepsilon_x} = \frac{y}{[d-y]}$$

$$\Rightarrow \varepsilon_c = \varepsilon_x \frac{y}{[d-y]}$$

From force equilibrium condition as shown in figure 3-4

$$T = C_s + C_c$$

Where :- C_c is the force in the compressed section of concrete

C_s is the force in the compression zone

T is the force in tension steel.

$$Cc = \int_0^x 20.95[2\ \frac{y}{d-y}\ \varepsilon_y + \frac{y^2}{[0.4-y]^2}\ \varepsilon x^2\ dy$$

$$= 30[-y \ln|d-y| - (d-y)\ln|d-y| + (d-y)\ ]_0^y - 11.25\left[\frac{y}{(d-y)}^2 + 2y \ln\ (d-y)\right.$$

$$+\ 2(d-y)\ \ln|d-y| - 2(d-y)]\ \Big|_0^y$$

The beam width is 0.3m. Therefore,

$$Cc = 10[0.4 \ln|d-y| -\ y\ - 0.366] - 3.38[\frac{y^2}{[d-y]^2} + 0.8 \ln|d-y| + 2\,y\ + 0.733]$$

$$\Rightarrow\ [-6.7\ \ln|0.4-y| - 16\ y\ - 6.13 - 3.38\frac{y^2}{0.4-y}\times 10^{-6}\ ]N\ \ \text{..... (i)}$$

The net force in the steel is :-

$F_s = T - C_s = A_s f_y - A' f_s$, but F_s is not known

$F_s = \varepsilon_s E_s$, $\varepsilon_s = \frac{kd - 0.0043}{kd}$ .....from triangular similarity

$$\Rightarrow \quad \frac{kd-0.0043}{kd}\ \frac{k}{1-k}\ \varepsilon x$$

$$F_s = 1407 \times 300 - 1127 \times 200{,}000\ [\ \frac{kd-0.0043}{kd} \text{x} \frac{k}{1-k}\ ] \text{x} 0.0015$$

$$F_s = 0.422 - 0.338\frac{Kd-0.0043}{d(1-K)}\ \text{MPa}$$

Therefore, from equilibrium equation :-

$F_c = F_s$

$$\Rightarrow\ -6.7\ln|d-y| - 16y - 6.13\frac{3.38y^2}{[d-y]} = 0.422 - \frac{0.338Kd-0.0043}{0.4(1-K)}$$

By trial and error,

y = 12.5 cm

From the strain diagram;

$$\varepsilon_c = \frac{y}{d-y}\,\varepsilon_s = \frac{0.125}{0.4-0.125}\times 0.0015 = 0.00682$$

The stress in the concrete is;

$$F_c = \varepsilon_c E_c = 0.00682(29\times 10^9) = 19.78MPa = 0.944\,fck$$

$$\varepsilon_{sc} = \frac{Kd-d'}{Kd}\,\varepsilon_c = \frac{Kd-0.043}{Kd}\,\varepsilon = \frac{0.125-0.043}{0.125}\times 0.000682$$

$$= 0.000447$$

$$F_{sc} = 0.000447\times 200GPa\times As = 84.48\times 10^6\times 1127\times 10^{-6}$$

$$F_{Sc} = 100.84KN$$

$$F_c = -6.7\ln|d-y| - 16y - 6.13\frac{3.38y^2}{[d-y]}\times 10^6\,N$$

$$F_c = 328KN$$

The total compressive force;

$$= 328 + 100.84 = 428.84KN$$

$$\bar{y}_{bot} = \frac{100.84*43 + 328*5/12*125}{428.84} = 49.95mm$$

$$jd = d - \bar{y}_{bot} = 357 - 49.95 = 307.05mm$$

$$M_y = A_s f_y jd = 1407*300*0.307 = 129.6KNm$$

$$\chi = \frac{f_y/E_s}{d-kd} = \frac{300/200*10^3}{357-125} = 6.465*10^{-6}\,rad/mm$$

$$\Rightarrow 6.465*10^{-3}\,rad/m = \theta$$

At the beginning of strain hardening of tensile steel ;

$\varepsilon_{su} = 0.015$ but the steel in compression has not yielded.

Steel under compression;

$$F_{sc} = \varepsilon_{sc'} E_s A_s = \varepsilon_{s'}[200*10^9*1127*10^{-6}]$$

$$\varepsilon s' = \frac{y-0.043}{0.4-y}\ \varepsilon_u \quad = \quad \frac{y-0.043}{0.4-y} * 0.015$$

$$\Sigma F_X = 0 \Rightarrow Fc = Fs - Fs'$$

$$Fc = -6.7\ln|d-y| - 16y - 6.13\frac{3.38y^2}{[d-y]} = 0.563 - \frac{y-0.043}{0.4-y} * 03.38$$

By trial and error;

$$Y = 0.081 = 8.1cm$$

Thus, $$\varepsilon_{s'} = \frac{y-0.043}{0.4-y}0.015 = \frac{0.081-0.043}{0.4-0.081}0.015$$

$$\varepsilon_{s'} = 0.001787$$

⇨ The steel in compression has yielded

Therefore,

$$F_s = 0.0015\ [200 \times 10^9 \times 1407 \times 10^{-6}] + [0.045 - 0.0015\ ]$$
$$[2.3 \times 10^9 \times 1407\ ] = 563\ KN$$

$$F_{s'} = 0.001787[200 \times 10^9 \times 1127 \times 10^{-6}] = 402.75KN$$

$$F_c = -6.7\ln|d-y| - 16y - 6.13\frac{3.3y^2}{[d-y]} = 155KN$$

$$F_c + F_{s'} \approx F_s \Rightarrow 155 + 402.75 \approx 563KN$$

The small discrepancy is due to the neutral axis depth approximation.

$$\overline{Y}_{bot} = \frac{402.75(43) + 155(0.375 \times 81)}{563} = 39.12mm$$

$$= jd = d - \overline{y}_{bot} = 357 - 39.12 = 317.88mm$$

$$M_u = A_s f_y jd = 1407 \times 300 \times 0.31788 = 178.97KNm$$

$$\psi = \frac{f_u / E_s}{d - kd} = \frac{0.045}{357 - 81} = 163 * 10^{-6}\ rad/mm$$

$$\theta = 163 * 10^{-3}\ rad/m$$

The results is presented in graphical form, along with SAP result, to show the different stages of stress that is at first crack of concrete, at first yield of reinforcement bar under tension and at the ultimate state of reinforcement bar. At the ultimate stage of tension bar, the compression bar has also yielded.

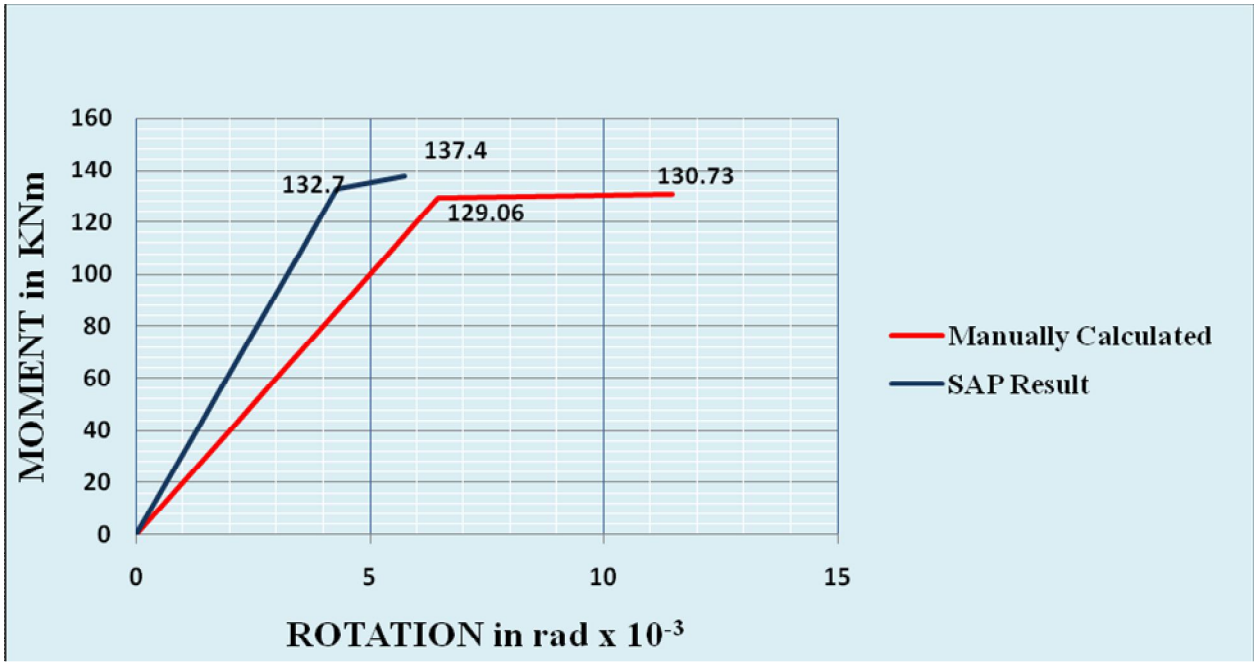

Figure 3-5 Comparison of results of SAP and Analytical Result

The above analytical calculation is used to verify the output of SAP analysis that is obtained from user defined fiber model of similar section used in the manual calculation as shown in Figure 3-5. Considering the axial load interaction and discrete fiber modeling in SAP, the result is in good agreement with the analytical calculation. The stiffness is larger in SAP analysis as could be expected due to axial load interaction and a finite number of discretized section.

3-5 Result Discussion

The result of SAP2000 [16] output is presented and discussed in the following order. One bay three storey, four storey, five storey and six storey results will be presented in table and graphs. Next, results of three bay frame with similar number of storey as the one bay frames will be discussed referring to tabular form presentation to show the relative values of storey drift, base

shear, base over turning moment, frame shear and moment at the interface of storey of the two class concretes. Results of one bay and three bay are presented in appendix B in tables. Finally results of six bay six storeys are assessed.

3-5-1 One bay frame

Possible plastic hinge zones are shown in figure 3-6 with 40cm hinge length. A plastic hinge length equal to the depth of the beam section is recommended for designs based on ductility class low. Hinge property derived from section fiber of members sections is used in defining the moment rotation relation. Hinge result for column member 1 is as shown in figure 3-7.

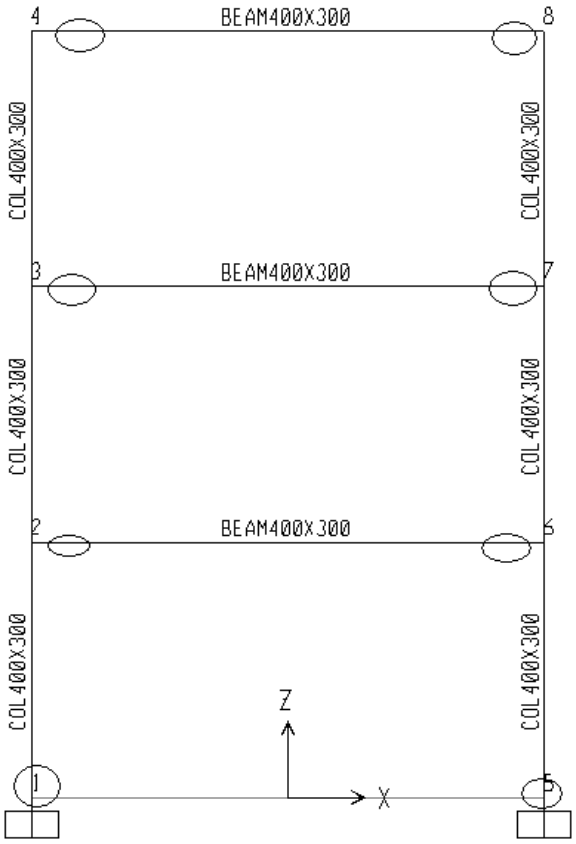

Figure 3-6 One bay three storey frame with possible plastic hinge location

From figure 3-7, hinge number one has attained a maximum moment and rotation of 115.45KNm and 0.00185radian respectively at 8.1 second this corresponds to the maximum displacement of joint 2 at the same time as shown in figure 3-8.

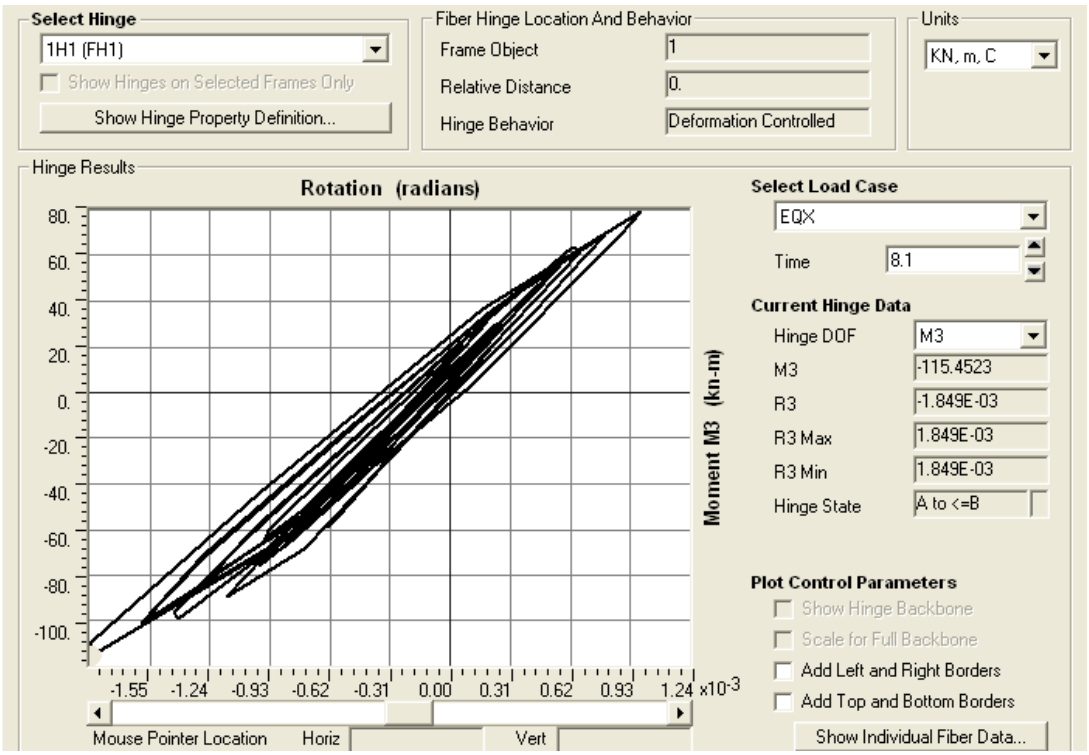

Figure 3-7 Hinge result for hinge number one

The absolute maximum displacement of joint 2 is the storey drift of the first storey since it is the relative value to the ground displacement. Hence, the drift to storey height ratio is (1.353cm /300cm) * 100%= 0.451% whose any of the fibers comprising this section has not yielded and it is in good agreement with Elnashai's recommendation[5]. He asserted that structural systems tend to behave linearly under low-magnitude earthquakes; at this stage, values of drift vary between 0.5% and 1%. Analytical work by Ashciem (2000) has shown that the yield horizontal displacement of steel moment resisting frames may vary between 1.0% and 1.2% of the height of the structure, while reinforced concrete frames often yield at about half of the above values [5].

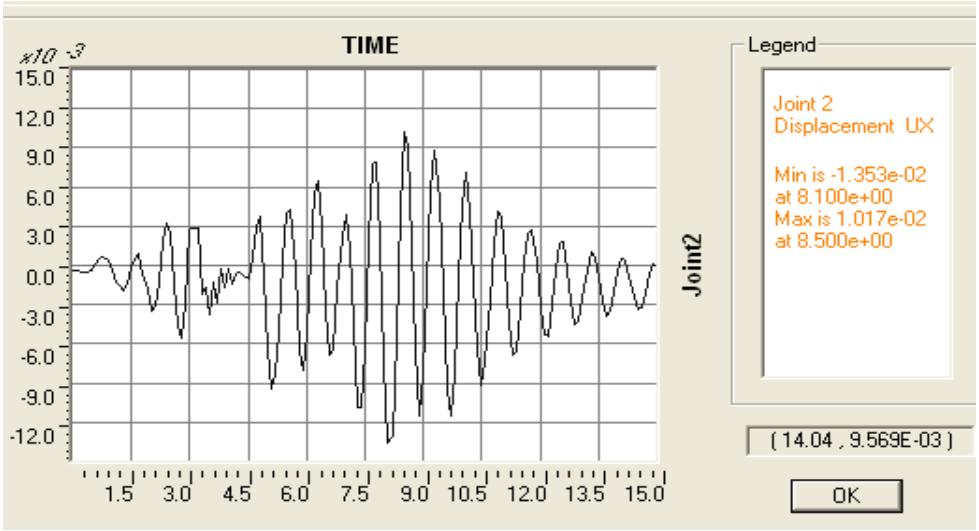

Figure 3-8 First storey displacement

Fiber result of section taken from hinge 2 in figure 3-9 shows that reinforcement bar at the corner of the beam section has yielded and has attained to the maximum of yield plateau but not reached to strain hardening stage. This could be observed by comparing the maximum axial strain of fiber number 4 whose strain is 0.0104m/m with 0.0015 which is the yield strain just at the beginning of strain hardening. In addition the strain is closer to 0.015 of backbone curve that corresponds to beginning of strain hardening point.

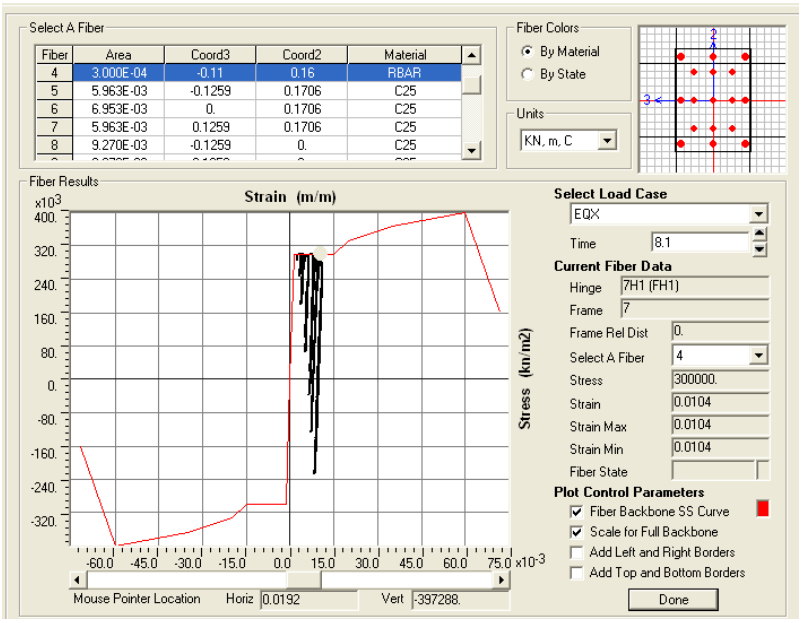

Figure 3-9 Fiber result of fiber 4 beam hinge 2.

Summary of results of the different comparing parameters for one bay three storey frame are presented in the table below with discussion of the outputs. The remaining four to six storey results are shown in appendix B. In three bay frames local and global effects are assessed through graphs. In addition, other outputs are presented in compacted form with only percentage difference from uniform class concrete is compared with one bay and six bay results. Storey drift, member moment and member shear are selected at the interface of the two concrete class. It is selected after assessing the comparatively larger difference in response from the uniform class. In this regard, storey drift difference is significant at the weaker storey just next to the interface unlike member shear and moment that attains the maximum deviation from the uniform class frame on the stronger side of the interface. In addition, comparison is made only on the absolute terms of maximum values so that higher percentages differences corresponding to the minimum results are neglected though it is much higher than their maximum counterparts.

							Percentage Difference			
		Uniform(A)	33% HC (B)	66% HC (C)	33% LC (D)	66% LC (E)	(A-B)/A	(A-C)/A	(A-D)/A	(A-E)/A
Base Shear (KN)	Minimum	-86.18	-87.50	-84.23	-84.64	-86.59	-1.53	2.26	1.79	-0.48
	Maximum	86.92	93.72	92.90	91.22	90.10	-7.82	-6.88	-4.95	-3.66
Base Moment (KNm)	Minimum	-618.90	-628.70	-621.50	-610.20	-624.30	-1.58	-0.42	1.41	-0.87
	Maximum	600.80	633.50	624.90	615.30	613.10	-5.44	-4.01	-2.41	-2.05
Member Shear 2 (KN)	Minimum	-49.26		-50.86	-50.88			-3.25	-3.29	
	Maximum	27.34		28.80	27.37			-5.34	-0.11	
Member Moment 2 (KNm)	Minimum	-63.33		-64.29	-63.26			-1.52	0.11	
	Maximum	44.98		51.56	43.88			-14.63	2.45	
Member Shear 3 (KN)	Minimum	-53.06				-53.92				-1.62
	Maximum	10.17				10.41				-2.36
Member Moment 3 (KNm)	Minimum	-61.85				-61.66				0.31
	Maximum	20.37				22.20				-8.98
3rd Storey Drift (cm/storey)	Minimum	-1.00		-1.09				-8.70		
	Maximum	1.46		1.52				-4.32		
2nd Storey Drift (cm/storey)	Minimum	-1.63	-1.77				-8.86			
	Maximum	1.78	1.86				-4.60			
1st Storey Drift (cm/storey)	Minimum	-1.35			-1.45				-6.87	
	Maximum	1.06			1.00				5.39	

Table 3-1 Summary of one bay three storey result

Note :- - HC : high class concrete
- 33% HC : higher concrete class is used for the bottom 33% of the storey
- LC : lower class concrete
- 33% LC: lower concrete class is used for the bottom 33% of the storey
- maximum values that are obtained at different response history of the frame.

One bay three storey frame

Increment in absolute maximum values of base shear and over turning moment is observed in the case of varied concrete class. Referring to table 3-1, the maximum increment for base shear and base overturning moment are 7.82% and 5.44% respectively. Comparison made on frame member shear and moment at the interface of the higher and lower class shows that an increment as high as 3.29% for shear and 1.52% for moment is recorded. Comparison made on storey drift just at the upper storey of the interface depicts that a maximum of 8.86% increment is observed. Significant difference is seen on the percentage when base moment is compared with storey moment and for shear also. The maximum difference on frame member shear and moment is observed on the stronger storey side of the interface while storey drift is maximum at the weaker side of the interface between the two classes of concrete.

One bay four storey frame

Table A-3-1 shows an increment in absolute maximum values of base shear though slight is noted. The maximum increments for base shear and base overturning moment being 1.69 % and -3.82%respectively. Comparison made on frame member shear and moment at the interface of the higher and lower class shows that an increment as high as 5.35% for moment and 9.15% for shear is recorded. Comparison made on storey drift just at the upper storey of the interface for case C depicts that a maximum of 11.11% increment is observed.

Significant difference is seen on the percentage differences when base moment is compared with member moment and for shear also. Stronger storey side of the interface shows maximum member shear and moment is maximum storey drift difference is recorded on the weaker side of the interface between the two classes of concrete. This effect as observed in frame member 3 and 10 columns that are located at the third and fourth storey.

One bay five storey frame

Though no significant difference is observed for base shear, overturning moment is observed to increase for varied concrete class as compared to the uniform concrete class. The maximum increments for base shear and base overturning moment being -0.94 % and 2.39% respectively. Comparison made on frame member shear and moment at the interface of the higher and lower class shows that an increment as high as 1.34% and 2.13% for shear and moment. Comparison made on storey drift shows no significant difference from the uniform class.

One bay six storey frame

In table A-3-3, increment in absolute maximum values of base shear and base overturning moment are observed to increase for varied concrete class as compared to the uniform concrete class. The maximum increments for base shear and base overturning moment are 6.17 % and 8.68% respectively. Comparison made on frame member shear and moment at the interface of the higher and lower class shows that an increment as high as 15.02% for shear and 16.91% for moment is obtained. Comparison made on storey drift shows a maximum of 13.18% increment is observed from that obtained from uniform class of concrete.

Significant difference is seen on the percentage when base moment is compared with storey moment and for shear also. This is observed at the stronger storey side of the interface while storey drift is maximum at the weaker side of the interface between the two classes of concrete.

3-5-2 Three bay moment resisting frame

The frame model, loading, hinge property, hinge location and material property are similar to one bay frame. The procedure of numerical method which is the Newmark's average acceleration method is used. Summary of results are presented in the next section along with the previous section's result and the succeeding six bay result to be discussed in the next section. The result is compiled in a single table 3-3 in which only the maximum percentage difference is shown for each category of parameters. Hence, one frame member moment and storey drifts value is taken for each case.

3-5-2-1 Effect assessment on global and local response

In this section the effect of concrete class variation both on local and global response will be assessed. The effect on global response is assessed by comparing base shear, percentage increments in base shear. The local effect is assessed by observing the results of column shear and column moment for the five cases. Additional case, that is, frame with 100% high class concrete is included in the comparison.

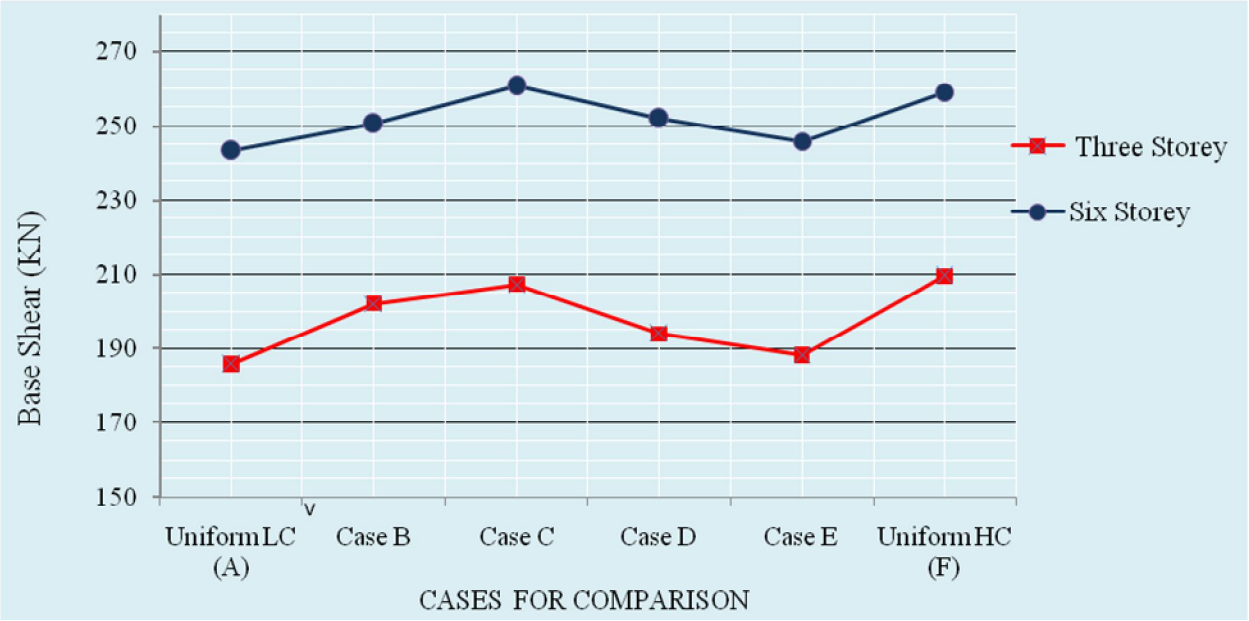

Figure 3-10 Base shear of three bay frames for the six cases

The base shear is larger for six storey than the three storey base shear as shown in figure 3-10. But maximum percentage increments for base shear are recorded in three storey frame especially for cases B,C and uniform high class F as shown in figure 3-11. The two storey show similarity which is a monotonous increment from case A to C and from case E to F. Similar trend of reduction in base shear is also observed from case C to E. Though a reduction is observed from case C to E, in all the five cases B to F, value higher than case A is obtained. Thus, figure 3-11 shows up to 12.81% increment in global response is observed in comparing base shear.

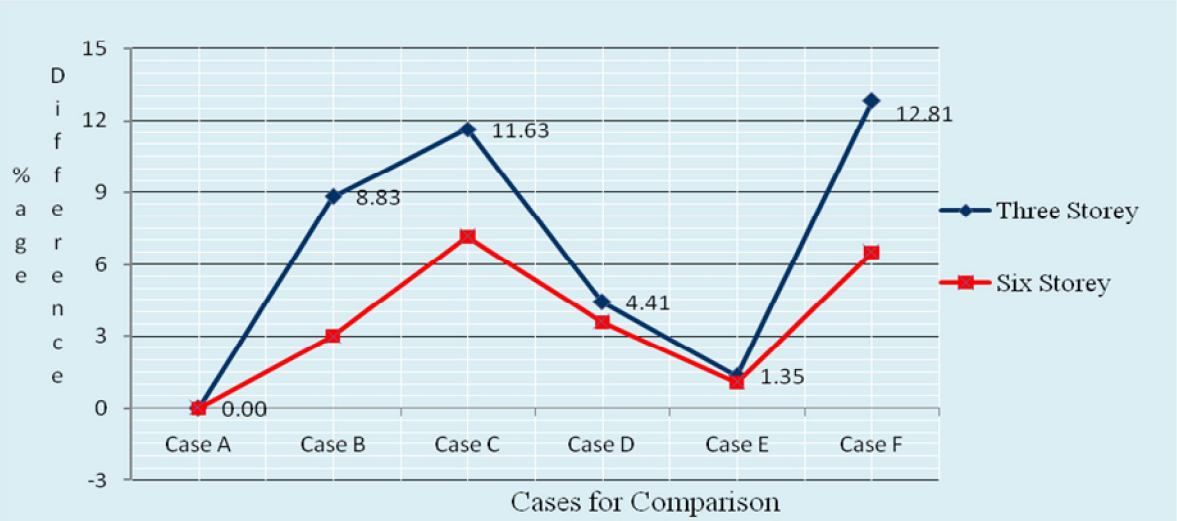

Figure 3-11 Percentage difference for base shear of three bay frames

Comparison made on column shear and column moment shows a general increase with number of storey. The increment is pronounced more for column moment as shown in figure 3-12

Figure 3-12 Percentage difference for column member moment of three bay frame

3-5-3 Six Bay moment resisting Frame

In this section, results of six bay moment resisting frame is assessed only for six storey frame. The effect of number of bay on global response is assessed by comparing percentage increment in base shear and storey drift. Time history of response in terms of for base shear and base overturning moments are presented since as it will be obvious later in table 3-3 that the difference is the maximum of all other case.

Maximum difference are encircled for maximum and minimum base shear. A maximum value of 529.0 - 449.9 = 79.1KN is observed from the positive shear whereas 381.5 -326.3 = 55.2 KN is the maximum increment for the negative values. The corresponding percentage difference are 16.20% and 19.07 % respectively. A relatively higher percentage increment is observed at different times that are shown encircled in figure 3-13 by circular loops but these values are not relevant as one is interested only at absolute maximum values for design purpose. Emphasis is given to the 16.2% increment as it is the absolute maximum value that arise due to utilization of high class concrete for the bottom 66% of the storey.

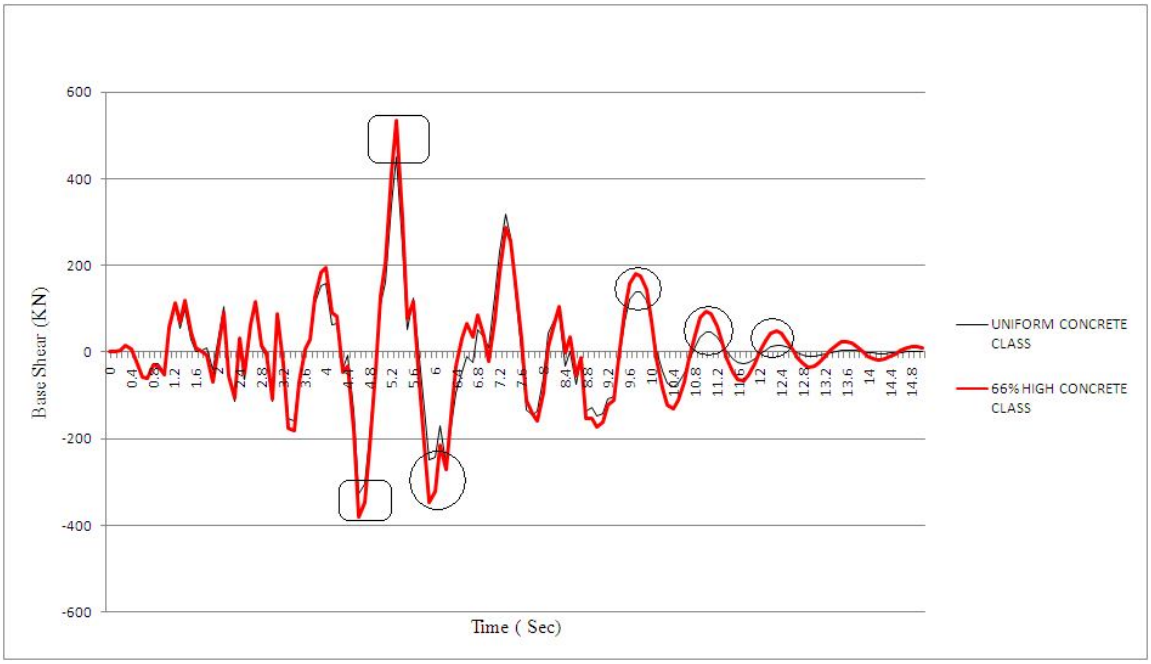

Figure 3-13 Base shear six bay six storey frame.

Here also maximum differences are encircled in figure 3-14 for maximum and minimum base moments. A maximum value of 5,880 - 4,818 = 1,062KNm is observed from the positive whereas 4,008-3,483 = 525KNm is the increment for the negative values. The corresponding percentage difference are 22.04 % and 15.07 % respectively. It is important to concentrate on the absolute maximum values irrespective of the sign as it is the design value. In this case emphasis should be given to the 22.04 % increment due to the base moment that

has increased from 4,818 to 5,880KNm. This is attributed to utilization of 41 MPa of concrete for the bottom 66% of the storey instead of C-25 concrete throughout the storey.

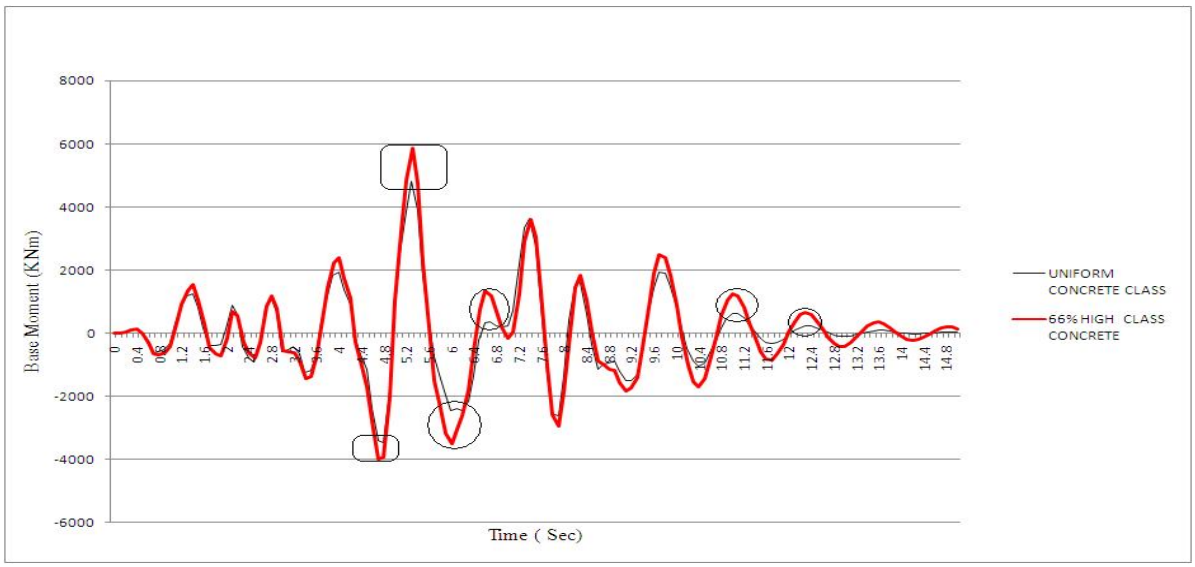

Figure 3-14 Base moment six bay six storey frame.

Percentage increment in base shear and storey drift are compared for one, three and six bay frames as shown in figure 3-15. Storey drift is chosen to be the maximum obtained irrespective of where it is observed. Though uniform trend of increment is not seen, an increment in general is observed with increase in number of bays.

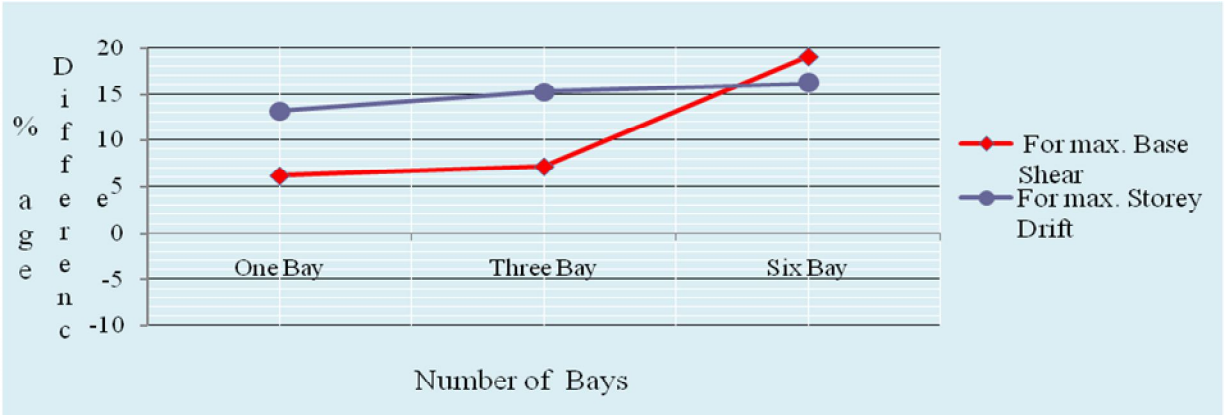

Figure 3-15 Percentage difference for base shear and drift of six storey frames

							Percentage Difference			
		Uniform(A)	33% HC (B)	66% HC (C)	33% LC (D)	66% LC (E)	(A-B)/A	(A-C)/A	(A-D)/A	(A-E)/A
Base Shear (KN)	Minimum	-326.30	-378.50	-381.50	-326.80	-324.20	-16.00	-16.92	-0.15	0.64
	Maximum	449.90	529.00	535.70	451.90	446.20	-17.58	-19.07	-0.44	0.82
Base Moment (KNm)	Minimum	-3,483.00	-3,972.00	-4,008.00	-3,520.00	-3,505.00	-14.04	-15.07	-1.06	-0.63
	Maximum	4,818.00	5,790.00	5,880.00	4,835.00	4,769.00	-20.17	-22.04	-0.35	1.02
Member Shear 80 (KN)	Minimum	-76.89	-84.22				-9.53			
	Maximum	16.27	13.55				16.72			
Member Moment 80 (KNm)	Minimum	-104.60	-116.50				-11.38			
	Maximum	12.58	16.05				-27.58			
Member Shear 81 (KN)	Minimum	-51.11	-55.61		-51.38		-8.80		-0.53	
	Maximum	4.21	0.70		1.80		83.37		57.24	
Member Moment 81 (KNm)	Minimum	-82.82	-89.22		-79.23		-7.73		4.33	
	Maximum	-17.27	-9.40		-8.59		45.57		50.26	
Member Shear 91	Minimum	-60.79	-64.35	-65.12			-5.86	-7.12		
	Maximum	-23.80	-21.21	-16.77			10.88	29.54		
Member Moment 91 (KNm)	Minimum	-87.73	-93.72	-93.27			-6.83	-6.31		
	Maximum	-36.45	-33.94	-29.07			6.89	20.25		
Member Shear 92 (KN)	Minimum	-68.74	-72.54			-71.36	-5.53			-3.81
	Maximum	-38.45	-35.37			-42.41	8.01			-10.30
Member Moment 92 (KNm)	Minimum	-96.31	-101.60			-100.50	-5.49			-4.35
	Maximum	-48.11	-41.59			-56.14	13.55			-16.69
Storey Drift 5 (cm/Storey)	Minimum	-0.71	-0.83	-0.82			-17.56		-16.15	
	Maximum	-0.28	-0.35	-0.33			-21.48		-14.79	
Storey Drift 4 (cm/Storey)	Minimum	-0.67	-0.82			-0.73	-21.64			-8.66
	Maximum	0.44	0.48			0.47	-8.64			-5.91
Storey Drift 3 (cm/Storey)	Minimum	-0.67	-0.79	-0.78			-16.99	-15.65		
	Maximum	0.62	0.67	0.58			-8.06	6.45		
Storey Drift 2 (cm/Storey)	Minimum	-0.73	-0.84		-0.77		-14.52		-4.93	
	Maximum	0.63	0.67		0.62		-6.35		1.90	

Table 3-2 Summary of Six Bay Six Storey Result

Finally results of all storeys are summarized in the following table to show the maximum difference. One value is selected from each category and the cases which attained the maximum values. It could be observed that uniform trend of increment is not observed. This could be attributed to the following factors:-

a- Different percentages of the storey height at which the concrete class changes is used for the practical reasons. For example, the five storey frame could take only one of the discrete values 20%,40%,60%& 80% other than totally being uniform whereas the three storey frame could take 33% or 66%. Therefore, comparison made for 33% case A of three storey as 20 or 40% case A of five storey frame would be inappropriate.

b- Various section sizes as obtained from equivalent static analysis are used for the different storey which obviously manipulates the response.

c- Member shear and moment are taken from different sections where maximum values are observed.

Case A does not appear in any of the summary. This implies that uniform frame output is exceeded in all the responses types, number of storey, and number of bay. The absolute maximum increment in base shear and base overturning moment is observed on six bay six storey frame. Maximum member shear and moment difference is noted on three bay four storey and one bay six storey frames respectively.

		ONE BAY FRAME				THREE BAY FRAME				SIX BAY FRAME
		Three storey	Four storey	Five storey	Six storey	Three storey	Four storey	Five storey	Six storey	Six storey
Base Shear (KN)	Case	B	B	A	C	C	D	C	C	C
	Maximum % age increased	7.82	1.69	0.00	6.17	11.63	1.04	1.78	7.15	19.07
Base Moment (KNm)	Case	B	E	B	C	C	C	C	C	C
	Maximum % age increased	5.44	0.76	2.39	8.68	11.66	10.15	5.79	7.99	22.04
Member Shear (KN)	Case	D	C	E	C	D	C	D	C	B
	Maximum % age increased	3.29	9.15	1.80	15.02	3.76	4.08	4.73	5.92	9.53
Member Moment (KNm)	Case	C	C	C	C	D	C	D	C	B
	Maximum % age increased	1.52	5.35	10.85	16.91	0.52	4.50	5.03	11.54	11.38
Storey Drift (cm/storey)	Case	B	E	D	C	C	C	E	E	B
	Maximum % age increased	8.86	0.21	0.46	24.92	13.70	32.18	1.05	15.28	21.64

Table 3-3 Summary of results

Note :-
Case A corresponds to uniform concrete frame
Cases B & C are 25%,33% or 40% of the bottom higher class concrete frames and 66%,75% or 80% of the bottom higher concrete class frames respectively.
Cases D & E are 25%,33% or 40% of the top higher class concrete frames and 66%,75% or 80% of the top higher concrete class frames respectively.

4-CONCLUSION

The parametric study was conducted for planar structures to reduce the variables involved and see the "targeted" effects of response. The variables involved were number of storey, number of bays, and percentage of the total storey at the interface of the two concrete classes. A step by step Newmark's numerical procedure is used in the analysis using SAP 2000. Higher class concretes are extracted from test results obtained from the mean plus one standard deviation value of actual test data of a total of 575 taken from 28^{th} day result.

From the analysis result the following observations should be noted:-

a- Higher response as compared to the uniform concrete class is observed in all cases.

b- A maximum increment in storey drift is 21.64%.

c- The base shear and base overturning moment has increased to the maximum by 19.07% & 22.04% respectively.

d- Member moment and member shear has increased to the maximum by 16.91% and 20.63% from that obtained in uniform class frames.

e- Considering Table 3-3 in general, higher values are observed for larger number of bays for all responses.

f- The difference in storey shear and moment is significant on the stronger storey of the interface while higher storey drift difference is observed on the weaker storey of the interface of the two concrete classes.

From the above observations, utilization of varied class of concrete has resulted in all the cases a higher response than the uniform counterparts. This implies that allowing the use of high class concretes in a given structure will bring about a higher stress or deflection than the initially calculated value during the design phase.

It should further be emphasized that the mean plus one standard deviation(41.06MPa) is the bases of our analysis. However, what if the absolute maximum test result which was 50MPa, that some samples attained among the data, instead of 41.06 MPa? Definitely the above difference would have been exaggerated.

With the above remarkable increment in all parametric cases and all response types selected for the research, it could be concluded that equal care should be taken in approving high quality test results as one should do for lower quality test results.

5 RECOMMENDATION

The present study is designed for planar moment resisting concrete frames. Distributed plastic hinge approach is selected in the analysis. At this point it would be wise to once again note the assumptions made. Perfect bond without bond slippage, shear deformation is neglected, infill participation is neglected and only moment resisting planar frames are included. The reason that the number of storey is limited to six is deeper sections were required without the incorporation of shear walls. Even the shallowest wall section will make the system frame equivalent dual system which is out of the thesis scope. This leads to analysis of dual lateral load resisting systems.

Therefore, future works considering the third dimensional effect would be of much help. Microscopic finite element model ,though time taking, has the power to assess the bond slippage, shear deformation, infill interaction and local damages thus closer and detailed result could be acquired.

Finally, the limitation on the number of storey would be lifted if dual systems or core systems are included.

REFERENCE

[1] Chopra, A. K. (1995), "Dynamics of Structures – Theory and Applications to Earthquake Engineering." Prentice Hall, Inc., Englewood cliffs, New Jersey.

[2] Cook, R.D.(1995)," Finite Element Modeling for Stress Analysis". A John Wiley & Sons Ltd., New York

[3] EBCS-2 (1995), "Structural use of concrete", Ministry of Works and Urban Development, Addis Ababa.

[4] EBCS-8 (1995), " Design of Structures for Earthquake Resistance ", Ministry of Works and Urban Development, Addis Ababa.

[5] Elnashai,A.S. and Sarno,L.D. (2008), "Fundamentals of Earthquake Engineering", A John Wiley & Sons Ltd., New York .

[6] European Committee for Standardization (2002), "Design of concrete structures," Euro-code 2 Part one 1 European Committee for Standardization", Brussels.

[7] Fillipou,F.C. and Issa,A. (1988),"Non Linear Analysis of Reinforced Concrete Frames Under Cyclic Load Reversals," Earth quake research center, college of engineering, university of California, Berkeley.

[8] Otani,S.(1980), "Nonlinear Dynamic Analysis of Reinforced Concrete Building Structures," Department of Civil Engineering, University of Toronto, Toronto, Ontario.

[9] Paz,Mario. (1985), "Structural Dynamics, Theory and Computation," Van Norstand Rienhold Company Inc., New York.

[10] Pecker, A. (2007), "Advanced earth quake engineering analysis," CISM, Udine Italy

[11] Penelis, G. G. and Kappos, A. J. (1997), "Earthquake Resistant Concrete Structures," St. Edmundsbury Press Limited, Bury St. Edmunds, Suffolk.

[12] Rashidi, J.Y., Darmon, R.A. and Dowell, R.K. (2004), "Recent Advances in Concrete Material Modeling and Application to the Seismic Evaluation and Retrofit of California Bridges".

[13] Troucer,F.F., Enrico, S.E. and Fillipou, F.C.(1991), "A Fiber Beam-Column Element for Seismic Response Analysis of Reinforced Concrete Structures", Earth quake research center, college of engineering, university of California, Berkeley.

[14] Wilson,E.L.(2000),"Three-Dimensional Static and Dynamic Analysis" Computer and structures, Inc., Berkeley, California.

[15] Zienkiewicz, O.C. and Taylor, R.L.(2000),"The Finite Element Method",Vol.2solid mechanics,5th edition, Butterworth-Hienemann.

[16] SAP 2000 version 14.2.0 Computers and Structures Inc. Berkeley, California.

APPENDIX A

Questionnaire to be filled by supervisors

This questionnaire is meant to be completed by the engineer or Engineer's representative. The aim of the questionnaire is to assess the response of the engineer towards concrete test result. The researcher, with due respect, request your cooperation. Your reply to the questionnaire would definitely benefit and would highly contribute to avoid biases that may occur in due course.

Put in the box corresponding to your answer

1. Educational Level

a. Diploma ☐ b. Advanced Diploma ☐ c. B.Sc. Degree ☐

d. M.Sc. and above ☐

2. Profession

Civil Engineer ☐ Building Engineer ☐ Architect ☐ Other _____

3. Specific Experience as a resident Engineer (site experience)

< 3 yrs ☐ 3 - 6 yrs ☐ 6 – 9 yrs ☐ 9 - 12yrs ☐ >12yrs ☐

4. State the category of your company you are working in

Category 1 ☐ Category 2 ☐ Category 3 ☐ Category 4 ☐ Category 5 ☐

5. Do you have a professional license?

Yes ☐ No ☐

6. Which one of the professional license do you have?

GE ☐ GAR ☐ GAE ☐ PST ☐ PAR ☐

PPST ☐ PPAR ☐ Other

7. How often do test results of materials are delivered for your checking?

_____

8. What is your response for concrete test result depicting higher class than required by the design? Do you accept?

Yes ☐ No ☐

If your answer is no, why?

_____

9. Do you think accepting such a result would always give a more safe structure?

   I think so ☐ No, I don't think so ☐

10. Have you ever thought that accepting high grade concrete (for example C-30 instead of C-25) could have a negative impact on action effects?

    Yes ☐ No ☐

APPENDIX B

		Uniform(A)	25% HC (B)	75% HC (C)	25% LC (D)	75% LC (E)	Percentage Difference		
							(A-B)/A	(A-C)/A	(A-D)/A	(A-E)/A
Base Shear (KN)	Minimum	-62.42	-62.22	-58.84	-61.23	-62.17	0.32	5.74	1.91	0.40
	Maximum	68.80	69.96	69.11	69.44	69.26	-1.69	-0.45	-0.93	-0.67
Base Moment (KNm)	Minimum	-514.70	-528.60	-536.60	-524.20	-519.70	-2.70	-4.25	-1.85	-0.97
	Maximum	563.40	561.40	541.90	563.70	567.70	0.35	3.82	-0.05	-0.76
Member Shear 2 (KN)	Minimum	-48.93			-48.08				1.74	
	Maximum	7.29			8.53				-16.96	
Member Moment 2 (KNm)	Minimum	-76.21			-75.21				1.31	
	Maximum	22.39			21.55				3.75	
Member Shear 3 (KNm)	Minimum	-41.99		-45.83				-9.15		
	Maximum	3.96		1.08				72.73		
Member Moment 3 (KNm)	Minimum	-66.96		-70.54				-5.35		
	Maximum	6.76		6.84				-1.18		
Member Shear 10 (KN)	Minimum	-50.00				-50.85				-1.70
	Maximum	23.60				24.60				-4.24
Member Moment 10 (KNm)	Minimum	-64.57				-64.65				-0.12
	Maximum	22.90				21.60				5.68
4th Storey Drift (cm/storey)	Minimum	-0.90		-0.80				11.11		
	Maximum	0.68		0.76				-11.18		
3rd Storey Drift (cm/storey)	Minimum	-1.45				-1.45				-0.21
	Maximum	0.97				0.98				-1.03
2nd Storey Drift (cm/storey)	Minimum	-1.61	-1.54				4.10			
	Maximum	1.03	1.08				-4.85			
1st Storey Drift (cm/storey)	Minimum	-1.12			-1.11				0.45	
	Maximum	0.47			0.50				-5.71	

Table A 3-1 Summary of one bay four storey result

		Uniform(A)	40% HC (B)	60% HC (C)	40% LC (D)	60% LC (E)	Percentage Difference			
							(A-B)/A	(A-C)/A	(A-D)/A	(A-E)/A
Base Shear (KN)	Minimum	-65.33	-60.86	-62.19	-61.44	-64.91	6.84	4.81	5.95	0.64
	Maximum	81.56	81.51	80.40	80.82	81.40	0.06	1.42	0.91	0.20
Base Moment (KNm)	Minimum	-471.30	-470.10	-463.20	-460.90	-471.70	0.25	1.72	2.21	-0.08
	Maximum	668.90	684.90	683.50	666.40	670.00	-2.39	-2.18	0.37	-0.16
Member Shear 2 (KN)	Minimum	-59.40	-58.63				1.30			
	Maximum	3.32	3.74				-12.65			
Member Moment 2 (KNm)	Minimum	-82.41	-80.92				1.81			
	Maximum	17.55	16.94				3.48			
Member Shear 3 (KN)	Minimum	-38.49		-37.45		-38.34		2.70		0.39
	Maximum	4.14		2.76		4.14		33.33		0.00
Member Moment 3 (KNm)	Minimum	-65.46		-65.93		-65.35		-0.72		0.17
	Maximum	5.91		3.63		6.02		38.58		-1.86
Member Shear 16 (KN)	Minimum	-49.16			-49.58				-0.85	
	Maximum	8.30			8.65				-4.22	
Member Moment 16 (KNm)	Minimum	-63.42			-67.89				-7.05	
	Maximum	11.79			10.60				10.09	
5th Storey Drift (cm/storey)	Minimum	-0.49		-0.49				0.20		
	Maximum	0.76		0.73				4.07		
4thStorey Drift 3 (cm/storey)	Minimum	-1.04				-1.04				-0.29
	Maximum	0.89				0.90				-1.12
3rd Storey Drift 2 (cm/storey)	Minimum	-1.10	-0.87				20.64			
	Maximum	0.87	0.89				-2.89			
2nd Storey Drift 1 (cm/storey)	Minimum	-1.10			-1.10				-0.46	
	Maximum	0.86			0.83				3.82	

A 3-2 Summary of one bay five storey result

							Percentage Difference			
		Uniform(A)	25% HC (B)	75% HC (C)	25% LC (D)	75% LC (E)	(A-B)/A	(A-C)/A	(A-D)/A	(A-E)/A
Base Shear (KN)	Minimum	-86.18	-90.27	-91.35	-89.05	-82.40	-4.75	-6.00	-3.33	4.39
	Maximum	97.67	96.57	103.70	97.69	97.67	1.13	-6.17	-0.02	0.00
Base Moment (KNm)	Minimum	-705.60	-681.40	-950.60	-707.00	-724.30	3.43	-34.72	-0.20	-2.65
	Maximum	976.30	980.90	1061.00	989.20	985.50	-0.47	-8.68	-1.32	-0.94
Member Shear 2 (KN)	Minimum	-76.33	-77.25				-1.21			
	Maximum	1.80	3.44				-91.11			
Member Moment 2 (KNm)	Minimum	-111.80	-116.40				-4.11			
	Maximum	11.30	7.22				36.11			
Member Shear 3 (KN)	Minimum	-52.57			-52.90				-0.63	
	Maximum	7.46			5.94				20.33	
Member Moment 3 (KNm)	Minimum	-82.70			-81.76				1.14	
	Maximum	8.07			3.66				54.65	
Member Shear 16 (KN)	Minimum	-62.43		-71.81				-15.02		
	Maximum	13.11		10.38				20.82		
Member Moment 16 (KNm)	Minimum	-83.58		-97.71				-16.91		
	Maximum	7.48		7.56				-1.07		
Member Shear 17 (KN)	Minimum	-51.80				-53.66				-3.59
	Maximum	9.17				12.45				-35.77
Member Moment 17 (KNm)	Minimum	-80.62				-86.16				-6.87
	Maximum	6.55				17.08				-160.76
Storey Drift 4 (cm/Storey)	Minimum	-0.60		-0.75				-24.92		
	Maximum	0.71		0.37				47.80		
Storey Drift 3 (cm/Storey)	Minimum	-0.71				-0.74				-5.08
	Maximum	0.62				0.66				-5.94
Storey Drift 2 (cm/Storey)	Minimum	-0.79	-0.82				-3.80			
	Maximum	0.72	0.66				8.33			
Storey Drift 1 (cm/Storey)	Minimum	-0.99			-1.02				-3.03	
	Maximum	0.83			0.78				5.55	

Table A 3-3 Summary of one bay six storey result

							Percentage Difference			
		Uniform(A)	33% HC (B)	66% HC (C)	33% LC (D)	66% LC (E)	(A-B)/A	(A-C)/A	(A-D)/A	(A-E)/A
Base Shear (KN)	Minimum	-182.90	-196.00	-199.30	-190.40	-185.30	-7.16	-8.97	-4.10	-1.31
	Maximum	185.80	202.20	207.40	194.00	188.30	-8.83	-11.63	-4.41	-1.35
Base Moment (KNm)	Minimum	-1,303.00	-1,402.00	-1,425.00	-1,351.00	-1,319.00	-7.60	-9.36	-3.68	-1.23
	Maximum	1,235.00	1,345.00	1,379.00	1,286.00	1,250.00	-8.91	-11.66	-4.13	-1.21
Member Shear 2 (KN)	Minimum	-47.58		-48.82	-49.37			-2.61	-3.76	
	Maximum	14.12		19.89	14.65			-40.86	-3.75	
Member Moment 2 (KNm)	Minimum	-56.27		-54.32	-56.56			3.47	-0.52	
	Maximum	34.62		46.41	34.47			-34.06	0.43	
Member Shear 3 (KN)	Minimum	-43.74				-44.04				-0.69
	Maximum	15.14				15.64				-3.30
Member Moment 3 (KNm)	Minimum	-56.11				-56.14				-0.05
	Maximum	24.44				23.94				2.05
3rd Storey Drift (cm/storey)	Minimum	-0.39		-0.44				-13.70		
	Maximum	1.18		1.29				-9.32		
2nd Storey Drift (cm/storey)	Minimum	-1.11	-1.21				-9.01			
	Maximum	0.65	0.72				-10.26			
1st Storey Drift (cm/storey)	Minimum	-1.27			-1.33				-4.49	
	Maximum	0.53			0.55				-4.76	

Table A 3-4 Summary of three bay three storey result

		Uniform(A)	25% HC (B)	75% HC (C)	25% LC (D)	75% LC (E)	Percentage Difference			
							(A-B)/A	(A-C)/A	(A-D)/A	(A-E)/A
Base Shear (KN)	Minimum	127.70	129.40	128.50	127.20	127.90	-1.33	-0.63	0.39	-0.16
	Maximum	182.20	183.70	182.30	184.10	182.50	-0.82	-0.05	-1.04	-0.16
Base Moment (KNm)	Minimum	-1,143.00	-1,217.00	-1,259.00	-1,211.00	-1,151.00	-6.47	-10.15	-5.95	-0.70
	Maximum	1,336.00	1,397.00	1,443.00	1,397.00	1,339.00	-4.57	-8.01	-4.57	-0.22
Member Shear 2 (KN)	Minimum	-46.87			-45.43				3.07	
	Maximum	3.99			4.16				-4.26	
Member Moment 2 (KNm)	Minimum	-57.31			-58.56				-2.18	
	Maximum	23.24			23.72				-2.07	
Member Shear 13 (KN)	Minimum	-44.11		-45.91				-4.08		
	Maximum	3.82		1.46				61.78		
Member Moment 13 (KNm)	Minimum	-58.04		-60.65				-4.50		
	Maximum	11.37		8.47				25.51		
Member Shear 10 (KN)	Minimum	-48.48				-49.08				-1.24
	Maximum	26.98				27.26				-1.04
Member Moment 10 (KNm)	Minimum	-66.08				-66.00				0.12
	Maximum	28.73				27.62				3.86
4th Storey Drift (cm/storey)	Minimum	-0.55		-0.45				17.03		
	Maximum	0.58		0.76				-32.18		
3rd Storey Drift (cm/storey)	Minimum	-1.08				-1.09				-0.93
	Maximum	0.80				0.79				0.63
2nd Storey Drift (cm/storey)	Minimum	-1.38	-1.40		-1.43		-1.38		-3.55	
	Maximum	0.73	0.71		0.70		2.74		4.11	
1st Storey Drift (cm/storey)	Minimum	-1.37								
	Maximum	0.27								

Table A 3-5 Summary of three bay four storey result

		Uniform(A)	40% HC (B)	60% HC (C)	40% LC (D)	60% LC (E)	Percentage Difference			
							(A-B)/A	(A-C)/A	(A-D)/A	(A-E)/A
Base Shear (KN)	Minimum	-164.70	-165.60	-163.60	-162.90	-164.50	-0.55	0.67	1.09	0.12
	Maximum	208.00	204.30	210.60	205.50	207.80	1.78	-1.25	1.20	0.10
Base Moment (KNm)	Minimum	-1,486.00	-1,625.00	-1,673.00	-1,577.00	-1,519.00	-9.35	-12.58	-6.12	-2.22
	Maximum	1,882.00	1,823.00	1,833.00	1,773.00	1,878.00	3.13	2.60	5.79	0.21
Member Shear 2 (KN)	Minimum	-75.76	-77.45				-2.23			
	Maximum	21.52	21.55				-0.14			
Member Moment 2 (KNm)	Minimum	-108.00	-111.90				-3.61			
	Maximum	16.28	16.43				-0.92			
Member Shear 13 (KN)	Minimum	-45.86		-48.03	-46.37			-4.73	-1.11	
	Maximum	1.11		0.86	0.83			22.52	24.95	
Member Moment 13 (KNm)	Minimum	-92.12		-96.75	-92.36			-5.03	-0.26	
	Maximum	2.14		3.12	3.39			-45.79	-58.41	
Member Shear 10 (KN)	Minimum	-60.00				-61.55				-2.58
	Maximum	19.59				20.64				-5.36
Member Moment 10 (KNm)	Minimum	-74.74				-75.85				-1.49
	Maximum	21.11				22.76				-7.82
5th Storey Drift (cm/storey)	Minimum	-0.25								
	Maximum	0.61								
4thStorey Drift (cm/storey)	Minimum	-0.95		-0.92					3.16	
	Maximum	0.60		0.56					6.67	
3rd Storey Drift (cm/storey)	Minimum	-0.78	-0.71			-0.78	9.44			0.51
	Maximum	0.98	0.97			0.98	1.02			0.00
2nd Storey Drift (cm/storey)	Minimum	-1.00			-1.01				-1.00	
	Maximum	0.80			0.79				1.13	

Table A 3-6 Summary of three bay five storey result

		Uniform(A)	33% HC (B)	66% HC (C)	33% LC (D)	66% LC (E)	Percentage Difference			
							(A-B)/A	(A-C)/A	(A-D)/A	(A-E)/A
Base Shear (KN)	Minimum	-178.40	-186.80	-191.10	-182.00	-179.40	-4.71	-7.12	-2.02	-0.56
	Maximum	243.40	250.70	260.80	252.10	246.00	-3.00	-7.15	-3.57	-1.07
Base Moment (KNm)	Minimum	-1,937.00	-1,958.00	-1,991.00	-1,961.00	-1,944.00	-1.08	-2.79	-1.24	-0.36
	Maximum	2,666.00	2,746.00	2,879.00	2,759.00	2,686.00	-3.00	-7.99	-3.49	-0.75
Member Shear 2 (KN)	Minimum	-79.60	-83.05				-4.33			
	Maximum	15.15	16.35				-7.92			
Member Moment 2 (KNm)	Minimum	-115.10	-121.70				-5.73			
	Maximum	12.22	17.48				-43.04			
Member Shear 3 (KN)	Minimum	-50.65			-51.07				-0.83	
	Maximum	3.18			3.80				-19.50	
Member Moment 3 (KNm)	Minimum	-93.45			-90.18				3.50	
	Maximum	18.82			19.74				-4.89	
Member Shear 16 (KN)	Minimum	-70.65		-74.83				-5.92		
	Maximum	21.18		24.02				-13.41		
Member Moment 16 (KNm)	Minimum	-110.90		-123.70				-11.54		
	Maximum	20.35		25.62				-25.90		
Member Shear 17 (KN)	Minimum	-44.76				-45.89				-2.52
	Maximum	12.34				13.55				-9.81
Member Moment 17 (KNm)	Minimum	-53.54				-54.38				-1.57
	Maximum	9.75				11.46				-17.54
5th Storey Drift (cm/Storey)	Minimum	-0.79		-0.68					13.92	
	Maximum	0.40		0.28					31.25	
4rth Storey Drift (cm/Storey)	Minimum	-0.72				-0.83				-15.28
	Maximum	0.54				0.59				-8.70
3rd Storey Drift (cm/Storey)	Minimum	-0.76		-0.78				-2.11		
	Maximum	0.65		0.58				11.18		
2nd Storey Drift (cm/Storey)	Minimum	-0.91			-0.93				-1.98	
	Maximum	0.68			0.68				0.58	

Table A 3-7 Summary of three bay six storey result